

Minimizing Surrogate Losses for Decision-Focused Learning using Differentiable Optimization

Jayanta Mandi^{a,*}, Ali İrfan Mahmutoğulları^a, Senne Berden^a and Tias Guns^a

^a KU Leuven, Department of Computer Science, Belgium

Abstract. Decision-focused learning (DFL) trains a machine learning (ML) model to predict parameters of an optimization problem, to directly minimize decision regret, i.e., maximize decision quality. Gradient-based DFL requires computing the derivative of the solution to the optimization problem with respect to the predicted parameters. However, for many optimization problems, such as linear programs (LPs), the gradient of the regret with respect to the predicted parameters is zero almost everywhere. Existing gradient-based DFL approaches for LPs try to circumvent this issue in one of two ways: (a) smoothing the LP into a differentiable optimization problem by adding a quadratic regularizer and then minimizing the regret directly or (b) minimizing surrogate losses that have informative (sub)gradients. In this paper, we show that the former approach still results in zero gradients, because even after smoothing the regret remains constant across large regions of the parameter space. To address this, we propose minimizing surrogate losses – even when a differentiable optimization layer is used and regret can be minimized directly. Our experiments demonstrate that minimizing surrogate losses allows differentiable optimization layers to achieve regret comparable to or better than surrogate-loss based DFL methods. Further, we demonstrate that this also holds for DYS-Net, a recently proposed differentiable optimization technique for LPs, that computes *approximate* solutions and gradients through operations that can be performed using feedforward neural network layers. Because DYS-Net executes the forward and the backward pass very efficiently, by minimizing surrogate losses using DYS-Net, we are able to attain regret on par with the state-of-the-art while reducing training time by a significant margin.

1 Introduction

Many real-world decision-making problems can be cast as combinatorial optimization problems. Some parameters of these optimization problems (e.g., production costs or travel times) are typically unknown due to uncertainty when the decisions are made. In the context of data-driven contextual optimization [27], the problems of predicting parameters of an optimization problem can be viewed as “predict-then-optimize” (PtO) problems, including two key steps—the *prediction* of the unknown parameters given the observed contextual information and the subsequent *optimization* using those predicted parameters. Decision-focused learning (DFL) [21] trains machine learning (ML) models to predict uncertain parameters by *directly* minimizing the decision loss, a measure of the quality of the decisions made using the predicted parameters.

Among ML models, neural networks have emerged as highly successful due to their ability to learn complex patterns from data [2]. However, training neural networks relies on gradient-based learning, which poses a fundamental challenge for DFL. Gradient-based DFL methods entail computing the partial derivatives of the optimization problem with respect to the predicted parameters. However, for combinatorial optimization problems, these partial derivatives are zero almost everywhere, since slight parameter changes rarely alter the solution, except at transition points, where the solution changes abruptly, and the partial derivatives do not exist. In this paper we consider combinatorial optimization problems which can be formulated as integer linear programs (ILPs) or mixed integer linear programs (MILPs). To obtain informative gradients for DFL on (MI)LPs, previous works employ two broad categories of approaches: (a) smoothing the (MI)LP into a differentiable optimization problem [34, 18, 13], and then minimizing the decision loss by differentiating through the ‘smoothed’ problem, or (b) using surrogate loss functions [12, 23, 20], for which informative gradients or subgradients exist.

Contribution. In this paper, we focus on the first category of DFL approaches. In this category, the (MI)LP is turned into a differentiable optimization problem as follows: the linear programming (LP) relaxation of the (MI)LP is first considered by removing the integrality constraints on the variables. Then, a quadratic regularizer is added to the objective to convert the LP into a quadratic program (QP). In practice, the smoothing strength is kept reasonably low to ensure that it does not overshadow the true objective of the original optimization problem. As mentioned earlier, approaches in this category minimize the decision loss on the training dataset by computing the Jacobian of the solution to the smoothed QP with respect to the predicted parameters using a differentiable solver (e.g., *Cvxpylayers* [1]). The motivation for minimizing decision loss on the training set follows the principle of empirical risk minimization (ERM) [32], which suggests that improvements on the training data should lead to lower decision loss on unseen test instances.

Our main argument is that direct minimization of decision loss using differentiable optimization is *ineffective* for gradient-based DFL. This is because QP smoothing makes the optimization problem differentiable by smoothing out abrupt transitions in the solution. However, this smoothing often leads to constant solutions across large regions of the parameter space. As a result, the gradient of the decision loss with respect to the predicted parameters becomes zero during back-propagation, rendering it ineffective for gradient-based DFL.

To overcome this challenge, we propose minimizing surrogate losses instead, even when direct minimization of the decision loss is feasible using a differentiable optimization layer. At first glance, this

* Corresponding Author. Email: jayanta.mandi@kuleuven.be

might seem counterintuitive: *Why would one optimize a surrogate loss when the decision loss can be directly minimized using a differentiable optimization solver?* We answer this question by demonstrating that the surrogate loss provides gradients that are useful for gradient-based training. We empirically demonstrate that minimizing the surrogate losses using differentiable optimization solvers provides gradients that lead to lower decision loss on unseen instances.

Furthermore, training in DFL is computation-intensive. Both types of approaches require solving the (smoothed) (MI)LP for each training instance with the predicted parameters in each epoch to compute the decision loss. This poses significant scalability challenges, and increases training time. To ease the computational burden, McKenzie et al. [22] recently developed a fully-neural optimization layer, DYS-Net. Unlike Cvxpylayers, DYS-Net computes the solution to the quadratically regularized LP and the gradient of the solution using neural operations such as matrix vector multiplications. By doing so, DYS-Net offers the potential to significantly speed up DFL training. However, this potential has not been fully established because McKenzie et al. [22] use datasets where the true parameters are *not* observed, while most DFL benchmarks [30] assume otherwise. So, DYS-Net has not been compared to the state-of-the-art DFL methods. We empirically show that minimizing surrogate losses with DYS-Net yields test-time regret comparable to state-of-the-art DFL methods, which *direct regret minimization cannot match due to the zero-gradient issue*. In summary, this paper makes the following contributions:

- We demonstrate that although ‘smoothing’ turns the (MI)LP into a differentiable optimization problem, the gradient of the empirical decision loss remains zero over most of the parameter space.
- We empirically show that for quadratic smoothing, minimizing surrogate losses leads to lower decision loss on test data than minimizing the decision loss.
- By minimizing the surrogate loss, using DYS-Net as the differentiable solver, we achieve decision loss comparable to state-of-the-art methods across three types of optimization problems, while significantly reducing training time (often by a factor of three).

2 Background

This work focuses on LPs, ILPs and MILPs. An LP can be represented in the following form:

$$\min_{\mathbf{w}} \mathbf{y}^\top \mathbf{w} \text{ s.t. } A\mathbf{w} = \mathbf{b}; \quad C\mathbf{w} \leq \mathbf{d}; \quad (1)$$

where $\mathbf{w} \in \mathbb{R}^K$ is a decision variable. The optimal solution for a given cost parameter, $\mathbf{y} \in \mathbb{R}^K$, is denoted by $\mathbf{w}^*(\mathbf{y})$. Note that any constraints in the form of $C\mathbf{w} \leq \mathbf{d}$ can be converted to equality by introducing slack variables and the LP can be transformed in the following standard form:

$$\min_{\mathbf{w}} \mathbf{y}^\top \mathbf{w} \text{ s.t. } A\mathbf{w} = \mathbf{b}; \quad \mathbf{w} \geq \mathbf{0} \quad (2)$$

For brevity, we use \mathcal{F} to denote the feasible space. So, for the standard LP formulation, $\mathcal{F} = \{\mathbf{w} \in \mathbb{R}^K \mid A\mathbf{w} = \mathbf{b}; \mathbf{w} \geq \mathbf{0}\}$. Unless it is explicitly stated otherwise, \mathbf{w}^* will denote $\mathbf{w}^*(\mathbf{y})$. ILPs differ from LPs in that the all decision variables \mathbf{w} are restricted to integer values. MILPs generalize ILPs by allowing only a subset of variables to be integer, while the rest can be continuous. Hence, MILPs can be seen as a superset that includes both LPs and ILPs. Although we describe our approach for MILPs, it naturally applies to ILPs and LPs as well.

We consider PtO for MILPs, where the vector of cost parameters \mathbf{y} is to be predicted using a vector of contextual information $\boldsymbol{\psi}$, correlated with \mathbf{y} . PtO problems comprise two steps: predicting unknown

parameters given contextual information and solving the MILP with these predicted parameters. In PtO problems, an ML model, \mathcal{M}_θ (with trainable parameters θ), is trained using past observation pairs $\{(\boldsymbol{\psi}_i, \mathbf{y}_i)\}_{i=1}^N$ to map $\boldsymbol{\psi} \rightarrow \mathbf{y}$. Due to their successful performance in many predictive tasks, neural networks are commonly used as the predictive model in PtO settings [34]. We denote the predicted cost produced by the neural network, as $\hat{\mathbf{y}}$, i.e., $\hat{\mathbf{y}} = \mathcal{M}_\theta(\boldsymbol{\psi})$.

A straightforward approach to the PtO problem is to train \mathcal{M}_θ minimize the prediction error between \mathbf{y} and $\hat{\mathbf{y}}$. However, previous works [12, 19, 34] show that such a *prediction-focused approach* can produce suboptimal decision performance. By contrast, in DFL, the ML model is directly trained to optimize the decision loss, which reflects the quality of the resulting decisions. When only the parameters in the objective function are predicted, the decision loss of interest is typically the *regret*, which measures the suboptimality of a decision resulting from a prediction. In DFL, one can consider other decision losses (Appendix A), such as squared decision errors (SqDE) between \mathbf{w}^* and \mathbf{w} . *Regret* and SqDE can be written in the following form:

$$\text{Regret}(\mathbf{w}, \mathbf{y}) := \mathbf{y}^\top \mathbf{w} - \mathbf{y}^\top \mathbf{w}^*, \quad \text{SqDE}(\mathbf{w}, \mathbf{y}) := \|\mathbf{w}^*(\mathbf{y}) - \mathbf{w}\|^2$$

The DFL approach trains \mathcal{M}_θ by minimizing $\frac{1}{N} \sum_{i=1}^N \text{Regret}(\mathbf{w}^*(\mathcal{M}_\theta(\boldsymbol{\psi}_i)), \mathbf{y}_i)$, the empirical risk minimization counterpart of $\mathbb{E}[\text{Regret}(\mathbf{w}^*(\mathcal{M}_\theta(\boldsymbol{\psi})), \mathbf{y})]$. This minimization of regret in gradient descent-based learning requires backpropagation through the optimization problem, which involves computing the Jacobian of $\mathbf{w}^*(\hat{\mathbf{y}})$ with respect to $\hat{\mathbf{y}} = \mathcal{M}_\theta(\boldsymbol{\psi})$. While $\frac{d\mathbf{w}^*(\hat{\mathbf{y}})}{d\hat{\mathbf{y}}}$ can be computed for convex optimization problems through implicit differentiation [1, 3], it raises difficulties when the optimization problem is combinatorial. This is because when the parameters of a combinatorial optimization problem change, the solution either remains unchanged or shifts abruptly, meaning the gradients are zero almost everywhere, and undefined at transition points.

There are two primary approaches to implementing DFL for MILPs: (a) smoothing the MILP to a differentiable convex optimization problem, and (b) using a surrogate loss that is differentiable. We briefly explain these approaches below. For more details on DFL techniques, we refer to the survey by Mandi et al. [21].

2.1 Differentiable Optimization by Smoothing of Combinatorial Optimization

To address the zero-gradient issue, methodologies in this category modify the optimization problem into a differentiable one by ‘smoothing’ and then analytically differentiating the smoothed optimization problem (see Appendix B for a detailed explanation). For LPs, Wilder et al. [34] propose transforming the LPs into ‘smoothed’ QPs by augmenting the objective function with the square of the Euclidean norm of the decision variables. Formally, they solve the following quadratically regularized QP:

$$\min_{\mathbf{w}} \hat{\mathbf{y}}^\top \mathbf{w} + \mu \|\mathbf{w}\|_2^2 \text{ s.t. } A\mathbf{w} = \mathbf{b}; \quad \mathbf{w} \geq \mathbf{0} \quad (3)$$

Exact differentiable optimization of the QP. The QP problem can be solved using differentiable solvers, such as *OptNet* [3] or *Cvxpylayers* [1]. The QP smoothing approach has been applied in various DFL works [13, 14, 22]. Mandi and Guns [18] consider another form of smoothing by adding a logarithmic barrier term into the LP. When the underlying optimization problem is an MILP or ILP, smoothing of the LP resulting from the continuous relaxation of the (MI)LP is carried out. Note that smoothing is applied *only during training* to

enable backpropagation through the smoothed QP; during testing and evaluation, the true MILP is solved.

When a differentiable solver like Cvxpylayers solves the QP, it computes the exact solution and the exact derivative by solving the QP using interior-point methods, and then differentiating the optimality conditions (i.e., the KKT optimality conditions). This requires computationally intensive matrix factorization such as LU decomposition.

Approximate differentiable optimization by DYS-Net. A recent method called DYS-Net [22] avoids the computational cost by not computing the exact solution and the exact derivatives. To compute an approximation of the solution of Eq. 3, DYS-Net uses projected gradient descent [10]. However, projecting into the feasible space of an LP is itself a complex operation. This complex projection is avoided through a fixed-point iteration algorithm based on a three-operator splitting method [9]. This version does not perform exact projections, but approximate projections. Note, for standard form LPs, the feasible space can be expressed as:

$$\mathcal{F} \equiv \mathcal{F}_1 \cap \mathcal{F}_2 \text{ where } \mathcal{F}_1 \doteq \{A\mathbf{w} = b\} \text{ and } \mathcal{F}_2 \doteq \{\mathbf{w} \geq 0\}.$$

Although projecting directly into \mathcal{F} is a complex task, projecting only into \mathcal{F}_1 or \mathcal{F}_2 are much simpler tasks, as shown below:

$$P_{\mathcal{F}_1}(\mathbf{w}) \doteq \mathbf{w} - A^\dagger(A\mathbf{w} - b) \text{ and } P_{\mathcal{F}_2}(\mathbf{w}) \doteq \max\{0, \mathbf{w}\}$$

where A^\dagger is the pseudo inverse of A and \max operates element-wise. Cristian et al. [8] propose continuously iterating between $P_{\mathcal{F}_1}$ and $P_{\mathcal{F}_2}$. In contrast, McKenzie et al. [22] propose the following fixed-point iteration:

$$\mathbf{w}_{\iota+1} = \mathbf{w}_\iota - P_{\mathcal{F}_2}(\mathbf{w}_\iota) + P_{\mathcal{F}_1}((2 - \alpha\mu)P_{\mathcal{F}_2}(\mathbf{w}_\iota) - \mathbf{w}_\iota - \alpha\mathbf{y}) \quad (4)$$

which converges to $\mathbf{w}^*(\mathbf{y})$ as $\iota \rightarrow \infty$.

The first efficiency gain of DYS-Net comes from its use of this fixed-point iteration in the forward pass, to approximate the solution of Eq. 3. The second efficiency gain is achieved in the gradient computation in the backward pass. Instead of obtaining the exact derivative by computing the inverse of the Jacobian of the fixed-point iteration, they use Jacobian-free backpropagation [15], by replacing the Jacobian with an identity matrix. They show that this provides useful approximate gradients for backpropagation. This approximation turns Eq. 4 into a series of matrix operations which can be implemented using standard neural network layers. We denote the solution obtained by this method as $DYS(\mathbf{y})$. After obtaining the solution using DYS-Net, McKenzie et al. [22] minimizes $SqDE$ and backpropagates it through DYS-Net. In contrast, we will propose to minimize surrogate losses after getting the solution using DYS-Net.

2.2 Surrogate Losses for DFL

Surrogate loss functions are used for training in DFL because they are crafted to have non-zero (sub)gradients while also reflecting the decision loss – as regret decreases, surrogate loss functions decrease as well. We discuss two surrogate losses, which we will use later.

2.2.1 Smart Predict then Optimize Loss (SPO+)

The SPO+ loss [12], a convex upper bound of $Regret(\mathbf{w}^*(\hat{\mathbf{y}}), \mathbf{y})$, is one of the first and most widely used surrogate losses for linear objective optimization problems. Instead of minimizing $Regret$, they

propose to minimize $\mathcal{L}_{SPO+}(\mathbf{w}^*(\hat{\mathbf{y}}), \mathbf{y})$, a convex upper bound of the regret. $\mathcal{L}_{SPO+}(\mathbf{w}^*(\hat{\mathbf{y}}), \mathbf{y})$ can be expressed in the following form:

$$\mathcal{L}_{SPO+}(\mathbf{w}^*(\hat{\mathbf{y}}), \mathbf{y}) = (2\hat{\mathbf{y}} - \mathbf{y})^\top \mathbf{w}^* - (2\hat{\mathbf{y}} - \mathbf{y})^\top \mathbf{w}^*(2\hat{\mathbf{y}} - \mathbf{y}) \quad (5)$$

2.2.2 Contrastive Loss

Mulamba et al. [23] propose the following surrogate loss, $\mathcal{L}_{SCE}^{\hat{\mathbf{y}}}(\mathbf{w}^*(\hat{\mathbf{y}}), \mathbf{y})$ based on self-contrastive estimation (SCE) [17].

$$\mathcal{L}_{SCE}^{\hat{\mathbf{y}}}(\mathbf{w}^*(\hat{\mathbf{y}}), \mathbf{y}) = \hat{\mathbf{y}}^\top \mathbf{w}^* - \hat{\mathbf{y}}^\top \mathbf{w}^*(\hat{\mathbf{y}}) \quad (6)$$

Note that this loss is similar to \mathcal{L}_{SPO+} , except that $2\hat{\mathbf{y}} - \mathbf{y}$ is replaced with $\hat{\mathbf{y}}$. One shortcoming of this loss is that for linear objectives, its minimum, which is zero, can be achieved either when $\mathbf{w}^*(\hat{\mathbf{y}}) = \mathbf{w}^*$ or when $\hat{\mathbf{y}} = 0$. To prevent minimizing the loss by always predicting $\hat{\mathbf{y}} = 0$, they further propose the following variant for linear objectives:

$$\begin{aligned} \mathcal{L}_{SCE}^{(\hat{\mathbf{y}}-\mathbf{y})}(\mathbf{w}^*(\hat{\mathbf{y}}), \mathbf{y}) &= (\hat{\mathbf{y}} - \mathbf{y})^\top \mathbf{w}^* - (\hat{\mathbf{y}} - \mathbf{y})^\top \mathbf{w}^*(\hat{\mathbf{y}}) \\ &= \hat{\mathbf{y}}^\top \mathbf{w}^* - \hat{\mathbf{y}}^\top \mathbf{w}^*(\hat{\mathbf{y}}) + \mathbf{y}^\top \mathbf{w}^*(\hat{\mathbf{y}}) - \mathbf{y}^\top \mathbf{w}^*(\mathbf{y}) \end{aligned} \quad (7)$$

Because in this work we focus on linear problems, we will primarily refer to $\mathcal{L}_{SCE}^{(\hat{\mathbf{y}}-\mathbf{y})}$ and will henceforth simply denote it by \mathcal{L}_{SCE} , except when explicitly distinguishing between $\mathcal{L}_{SCE}^{\hat{\mathbf{y}}}$ and $\mathcal{L}_{SCE}^{(\hat{\mathbf{y}}-\mathbf{y})}$.

Nevertheless, computation of \mathcal{L}_{SPO+} or \mathcal{L}_{SCE} entails solving the MILP with the predicted $\hat{\mathbf{y}}$ for each training instance in every epoch leading towards a significant computational burden. Mandi et al. [19] propose to minimize the LP relaxation for computing \mathcal{L}_{SPO+} . Mulamba et al. [23] address the computational issue by using solution caching instead of repeatedly solving the MILP. The CaVE technique, proposed by Tang and Khalil [31] for ILPs minimize a different surrogate loss function, which avoids solving the problem during training by minimizing the angle between the predicted cost vector and the ‘normal cone’ of the true optimal solution.

3 The Gradients of Surrogate Loss Functions

In this work, we investigate the use of surrogate losses in decision-focused learning, even when a differentiable optimization solver is used. After smoothing the optimization problem, the regret can be minimized directly using the solution of this layer. However, we explore whether surrogate losses still offer advantages in this setting.

3.1 Surrogate Losses without Differentiable Optimization

Note that if we minimize \mathcal{L}_{SCE} or \mathcal{L}_{SPO+} using a non-differentiable solver, the solution, $\frac{\partial \mathbf{w}^*(\mathbf{y})}{\partial \mathbf{y}}$ cannot be computed. In this case, the SPO+ and SCE losses are minimized using gradients, $\nabla \mathcal{L}_{SPO+}$ and $\nabla \mathcal{L}_{SCE}$ respectively, which can be expressed as follows:

$$\nabla \mathcal{L}_{SPO+} = 2(\mathbf{w}^* - \mathbf{w}^*(2\hat{\mathbf{y}} - \mathbf{y})) \quad (8)$$

$$\nabla \mathcal{L}_{SCE} = (\mathbf{w}^* - \mathbf{w}^*(\hat{\mathbf{y}})) \quad (9)$$

We highlight that in such cases $\mathbf{w}^*(\hat{\mathbf{y}})$ will be treated as a constant for gradient computation. Because of this reason, and the gradient of $\mathcal{L}_{SCE}^{(\hat{\mathbf{y}}-\mathbf{y})}$ (7) would be same as the gradient of $\mathcal{L}_{SCE}^{\hat{\mathbf{y}}}$ (6). Hence, in the absence of a differentiable optimization layer, minimizing either of these losses by gradient descent results in the same outcome. Next we will compare between minimizing \mathcal{L}_{SPO+} and \mathcal{L}_{SCE} using a non-differentiable solver. First, we will show in Theorem 1 that turning

$\nabla \mathcal{L}_{SCE}$ or $\nabla \mathcal{L}_{SPO+}$ zero ensures that the solution to the true cost is an optimal solution to the predicted cost assuming that $w^*(y)$ is the unique solution for the true cost.

Theorem 1. Suppose $\mathcal{Y}_{SCE}(y) = \{\hat{y} : \nabla \mathcal{L}_{SCE}(w^*(\hat{y}), y) = 0\}$ and $\mathcal{Y}_{SPO+}(y) = \{\hat{y} : \nabla \mathcal{L}_{SPO+}(w^*(\hat{y}), y) = 0\}$. Then, $w^*(y)$ is an optimal solution to (2) for any $\hat{y} \in \mathcal{Y}_{SCE}(y)$ or $\hat{y} \in \mathcal{Y}_{SPO+}(y)$. (Proof is provided in Appendix C.1)

Next, we present Theorem 2, which shows that minimizing \mathcal{L}_{SPO+} results in predicted cost parameters \hat{y} that are more robust to perturbations, compared to minimizing \mathcal{L}_{SCE} under the uniqueness assumption of the solution.

Theorem 2. For any $\hat{y} \in \mathcal{Y}_{SCE}(y)$ or $\hat{y} \in \mathcal{Y}_{SPO+}(y)$, we define the perturbation threshold as the norm of the smallest perturbation Δ such that $w^*(y)$ is no longer an optimal solution to $\hat{y} + \Delta$. Formally,

$$\Gamma(\hat{y}) := \min_{w' \in \mathcal{F}, \Delta} \|\Delta\|_2 \quad (10)$$

$$\text{s.t. } (\hat{y} + \Delta)^\top w^* > (\hat{y} + \Delta)^\top w'$$

Now let,

$$\Gamma_{SCE} := \min_{\hat{y} \in \mathcal{Y}_{SCE}(y)} \Gamma(\hat{y}), \quad \Gamma_{SPO+} := \min_{\hat{y} \in \mathcal{Y}_{SPO+}(y)} \Gamma(\hat{y}) \quad (11)$$

Then $\Gamma_{SPO+} \geq \Gamma_{SCE}$.

While the proof is provided in the Appendix C.2, we provide intuition for Theorem 2 with a simple example. Suppose that we have to select the most valuable of two items, with true values 5 and 10. Now, $\nabla \mathcal{L}_{SPO+} = w^*(2\hat{y} - y)$ becomes zero when the predicted value of the second item exceeds that of the first by at least half the difference in their true values, i.e., $(10 - 5)/2 = 2.5$. In contrast, $\nabla \mathcal{L}_{SCE}$ becomes zero as soon as the predicted value of the second item slightly exceeds that of the first, e.g., if the corresponding predictions are 8 and 8.01. With such predictions, $\nabla \mathcal{L}_{SCE}$ is already zero, and there is no gradient signal to make the difference any larger. In this way, minimizing \mathcal{L}_{SCE} with a non-differentiable solver can leave \hat{y} stuck near such *boundaries*, where slight perturbations yield a solution different from the true optimal.

3.2 Surrogate Losses with Differentiable Optimization

To use a differentiable solver, if the problem is an MILP, it is first relaxed to an LP. Moreover, the LP is non-smooth, as small changes in the cost parameter either leave the solution unchanged or cause abrupt shifts. QP smoothing converts the non-smooth LP into a smooth, differentiable QP, allowing regret to be computed and differentiated by solving the smoothed QP using a differentiable optimization layer. Existing DFL approaches under this category minimize the empirical regret of the smoothed problem, assuming that this reduces the expected regret on unseen instances. However, through a close inspection of how the incorporation of smoothing changes the gradient landscape, we reveal a shortcoming in this approach.

The introduction of smoothing ensures that the solution transitions smoothly, rather than abruptly, near the original LP's transition points. However, the solution of the smoothed QP remains unchanged, or changes very slowly, in regions that are not near the transition points, provided that the smoothing strength is kept low as illustrated in Figure 7b in Appendix B. So, in this region, $\frac{dw^*(\hat{y})}{d\hat{y}}$ is nearly zero.

When regret is minimized, its derivative with respect to the \hat{y} takes the following form:

$$\left. \frac{\partial w^*(y)}{\partial y} \right|_{y=\hat{y}} y \quad (12)$$

where $\left. \frac{\partial w^*(y)}{\partial y} \right|_{y=\hat{y}}$ is computed by considering the smoothed optimization problem. Similarly, if SqDE were considered as the training loss, the derivative would be:

$$\left. \frac{\partial w^*(y)}{\partial y} \right|_{y=\hat{y}} (w^*(\hat{y}) - w^*) \quad (13)$$

As we illustrated above, smoothing addresses the non-differentiability at the transition points, but the derivative $\frac{dw^*(\hat{y})}{d\hat{y}}$ still remains zero far from these points. Hence, in both Eq. 12 and Eq. 13, the derivative remains zero across large regions of the parameter space, due to $\left. \frac{\partial w^*(y)}{\partial y} \right|_{y=\hat{y}}$ becoming zero. Consequently, training by gradient descent would fail to change \hat{y} despite \hat{y} resulting in non-zero regret.

To prevent the derivative from *vanishing far from the transition points*, in this paper, we argue in favour of minimizing a surrogate loss even when SqDE or Regret can be directly minimized using a differentiable solver. For instance, when \mathcal{L}_{SPO+} is minimized, the derivative of it after smoothing with respect to the \hat{y} would be:

$$2(w^* - w^*(2\hat{y} - y)) + 2 \left. \frac{\partial w^*(y)}{\partial y} \right|_{y=2\hat{y}-y} (y - 2\hat{y}) \quad (14)$$

Similarly if \mathcal{L}_{SCE} is minimized after smoothing, the resulting derivative would be:

$$(w^* - w^*(\hat{y})) + \left. \frac{\partial w^*(y)}{\partial y} \right|_{y=\hat{y}} (y - \hat{y}) \quad (15)$$

What sets Eq.14 and Eq.15 apart from Eq. 12 is the term $(w^* - w^*(\hat{y}))$. The term $(w^* - w^*(\hat{y}))$ prevents $\frac{d\mathcal{L}}{d\hat{y}}$ going to zero even when $\frac{dw^*(\hat{y})}{d\hat{y}} \approx 0$.

3.3 Numerical Illustrations

To illustrate that zero-gradient issue persists even after QP smoothing, we will demonstrate how the gradient landscape changes after QP smoothing with a simple illustration. For this, we consider the following one-dimensional optimization problem:

$$\min_w yw \quad \text{s.t. } 0 \leq w \leq 1 \quad (16)$$

where $y \in \mathbb{R}$ is the parameter to be predicted. Note that the solution of this problem is: $w^*(y) = 1$ if $y < 0$ and $w^*(y) = 0$ if $y > 0$; and $y = 0$ for any value in the interval $[0, 1]$ is an optimal solution. Let us assume that the true value of y is 4 and hence $w^*(y) = 0$. The red line in Figure 1 shows how regret changes with predicted \hat{y} : 4 when $\hat{y} \leq 0$ and 0 when $\hat{y} > 0$. The regret changes abruptly at $\hat{y} = 0$.

The solution after augmenting the objective with the quadratic smoothing term $\frac{\mu}{2} w^2$ with $\mu > 0$ is:

$$w^*(y) = \begin{cases} 0; & \text{when } y > 0 \\ -\frac{y}{\mu}; & \text{when } -\mu < y \leq 0 \\ 1; & \text{when } y \leq -\mu \end{cases}$$

The regret with the smoothed QP is shown by the yellow line in Figure 1 for $\mu = 6$. The smoothing makes the derivative non-zero in

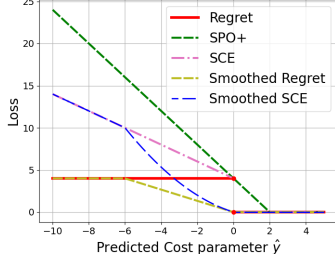


Figure 1: The numerical illustration shows that while smoothing causes solution plateaus with zero gradient. In contrast, \mathcal{L}_{SCE} (with or without smoothing) ensures a non-zero gradient when regret is non-zero.

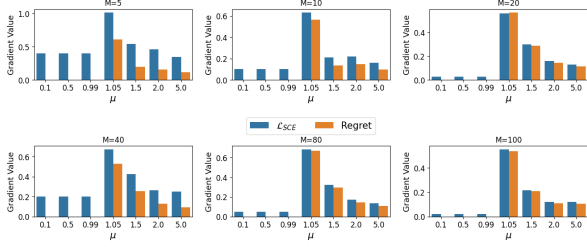


Figure 2: Results of computational simulation.

the interval $-\mu \leq y \leq 0$, but zero when $y < -\mu$. Note if $\hat{y} < -\mu$, the derivative of regret is 0, even if regret is non-zero. Hence, the predictions cannot be changed by gradient descent despite regret being zero. The smoothing strength can be increased by setting μ to a high value. However, if $\mu \gg |y|$, $w^*(y) \approx 0$ almost everywhere.

We plot \mathcal{L}_{SCE} with and without smoothing with blue and violet colors, respectively. In both cases, \mathcal{L}_{SCE} is strictly decreasing for $\hat{y} < 0$ ensuring a non-zero derivative for $\hat{y} < 0$ and guiding \hat{y} towards the positive half-space. The fact that minimizing regret leads to zero gradients, limiting gradient-based learning, is further evidenced on a 2-dimensional LP in Appendix D.

3.4 Impact of Differentiable Optimization on \mathcal{L}_{SCE}

In Section 3.1, we argue that minimizing \mathcal{L}_{SPO+} provides better robustness than minimizing \mathcal{L}_{SCE} with a non-differentiable solver. Recall that this is due to the fact that there is not much gradient signal to move away from the boundary when \mathcal{L}_{SCE} is minimized without differentiable optimization. However, minimizing with a differentiable solver can prevent this. In this case, if \hat{y} lies in such boundary, the term, $\frac{\partial w^*(y)}{\partial y} \Big|_{y=\hat{y}} (y - \hat{y})$ will be non-zero and this part of the gradient will push \hat{y} away from the boundary. On the other hand, if \hat{y} is far from the boundary and still $w^*(\hat{y}) \neq w^*$, the term, $\frac{\partial w^*(y)}{\partial y} \Big|_{y=\hat{y}} \approx 0$, but the first term of the gradient will drive \hat{y} to make $w^*(\hat{y}) = w^*$. In principle, both \mathcal{L}_{SCE} or \mathcal{L}_{SPO+} can be minimized using a differentiable solver. However, we want to highlight the following properties of \mathcal{L}_{SCE} in Proposition 1.

Proposition 1. For all, $y, \hat{y} \in \mathbb{R}^K$, the following holds:

1. $\mathcal{L}_{SCE}(w^*(\hat{y}), y) \geq 0$
2. When the set of optimal solutions is a singleton
 $\mathcal{L}_{SCE}(w^*(\hat{y}), y) = 0 \Leftrightarrow \text{Regret}(w^*(\hat{y}), y) = 0$.

(A proof is provided in Appendix C.3. We also show generalization bounds for \mathcal{L}_{SCE} loss in Appendix C.4.)

Proposition 1 shows that \mathcal{L}_{SCE} is zero whenever *Regret* is zero. However, \mathcal{L}_{SPO+} is an upper-bound of *Regret* and can be non-zero, even when *Regret* is zero. We can see this in Figure 1. Another consideration is that \mathcal{L}_{SPO+} is a convex loss even without smoothing, whereas \mathcal{L}_{SCE} is not, as it has discontinuity. However, it becomes a convex loss after smoothing. We will empirically investigate which one, after smoothing, is more useful for gradient-based DFL.

Further, note that if we minimize \mathcal{L}_{SCE} or \mathcal{L}_{SPO+} using a non-differentiable solver, $\frac{\partial w^*(y)}{\partial y}$ cannot be computed and only the first part of the derivative would be used. So, in such cases, Eq. 14 and Eq. 15 would reduce to SPO+ and SCE subgradients, respectively. We also mentioned in Section 3.1 that when $\mathcal{L}_{SCE}^{\hat{y}}$ and $\mathcal{L}_{SCE}^{(\hat{y}-y)}$ are minimized with a non-differentiable solver, they yield the same gradient. Note that this is not the case when using a differentiable solver. In that case, the gradient of $\mathcal{L}_{SCE}^{\hat{y}}$ differs from $\mathcal{L}_{SCE}^{(\hat{y}-y)}$, as shown below:

$$(w^* - w^*(\hat{y})) - \frac{\partial w^*(y)}{\partial y} \Big|_{y=\hat{y}} (\hat{y})$$

4 Simulation-Based Gradient Analysis on LPs

Through simulations on synthetically generated data, in this section, we will further demonstrate that the zero-gradient issue exists even for quadratically regularized LPs larger than one dimension. For the simulations, we consider Top-1 selection problems with different numbers of items M . This can be represented as the following LP:

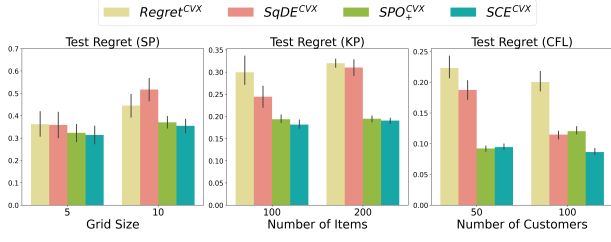
$$\max_{y \in \{0,1\}} y^\top w \quad \text{s.t. } w^\top \mathbf{1} \leq 1 \quad (17)$$

Here, $y = [y_1, \dots, y_M] \in \mathbb{R}^M$ is the vector denoting value of all the items and $w = [w_1, \dots, w_M]$ is the vector of decision variables. To replicate the setup of a PtO problem, we solve the optimization problem with \hat{y} , compute *Regret* and \mathcal{L}_{SCE} , and then analyze the corresponding gradients. To generate the ground truth y , we randomly select M integers without replacement from the set $\{1, \dots, M\}$. The predicted costs, \hat{y} , are generated by considering a different sample from the same set. As a result, y and \hat{y} contain the same numbers but in different permutations. We solve the LP with \hat{y} , after adding the quadratic regularizer μ , using Cvxpylayers.

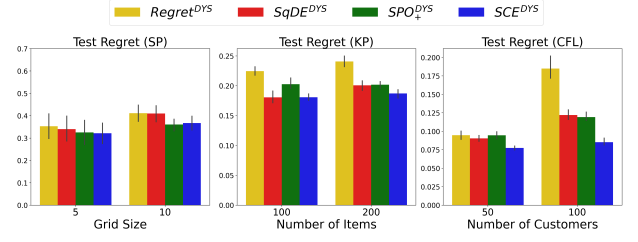
We compute the gradients of *Regret* and \mathcal{L}_{SCE} for multiple values of M and μ . For each configuration of M and μ , we run 20 simulations, and show the average absolute values of the gradients of the two losses – \mathcal{L}_{SCE} and *Regret* – in Figure 2. We also show the average Manhattan distance between solutions of the true LP and ‘smoothed’ QP for same \hat{y} in Table 1. As we hypothesized, the gradient turns zero whenever *Regret* is minimized with $\mu < 1$. This is not the case when \mathcal{L}_{SCE} is minimized. We refer readers to Appendix D for a detailed description of the simulation setup and analysis.

Table 1: We tabulate average Manhattan distance between the the LP and the smoothed QP solutions for different values of M and μ .

μ	M					
	5	10	20	40	80	100
0.100	0.000	0.000	0.000	0.000	0.000	0.000
0.500	0.000	0.000	0.000	0.000	0.000	0.000
0.990	0.000	0.000	0.000	0.000	0.000	0.001
1.050	0.089	0.089	0.089	0.089	0.089	0.089
1.500	0.465	0.466	0.465	0.465	0.465	0.464
2.000	0.622	0.622	0.622	0.622	0.622	0.622
5.000	1.165	1.165	1.165	1.165	1.165	1.165



(a) Cvxpylayers



(b) DYS-Net

Figure 3: Minimizing surrogate losses versus *Regret* or *SqDE* using differentiable optimization.

5 Experimental Evaluation

We will consider the following three optimization problems in our experiments. We provide detailed descriptions and mathematical formulations in Appendix F. See Appendix H for hyperparameters and tabulated results.¹

Shortest path on a grid (SP). The goal of this optimization problem is to find the path with lowest cost on a $k \times k$ grid, starting from the southwest node and ending at the northeast node of the grid [12]. A SP problem is characterized by the size of the grid, k . The cost of each edge is unknown and should be predicted before solving the problem. This problem can be solved as an LP, due to total unimodularity [35].

Multi-dimensional knapsack (KP). In this problem, a maximal value subset of items must be selected while respecting two-dimensional capacity constraints. The weights and capacities are known, and the item values should be predicted. Each KP instance is defined by the number of items. The problem is an ILP.

Capacitated facility location (CFL). Given a set of feasible facility sites and a set of customers, the goal is to satisfy the customers' demands for a single product while minimizing the total cost. The total cost includes both the fixed costs of opening the facilities and the transportation costs. The fixed costs, customer demands, and facility capacities are assumed to be known. In the PtO version, the transportation costs are considered unknown. The problem is a MILP.

5.1 Experimental Setup

The training, validation and test instances for the SP, KP and CFL problems are generated using PyEPO [30]. In all problems considered, the true relationship between features ψ and costs y is non-linear, but we use linear models to predict y . This setup, common in PtO evaluations, highlights how DFL methods can still achieve low regret even when the predictive model is misspecified. Appendix F.2 explains the true underlying relationship between the cost and the features. We use the polynomial degree parameter and the noise half-width parameter as 6 and 0.5, respectively, in all our experiments. The predictive models are implemented using PyTorch [25], and Gurobipy [16] is used to implement the (MI)LPs. For evaluation, we always compute the optimal solution both for true and predicted costs using the (MI)LP solvers. For all the experiments, we report the average of *normalized relative regret* on test instances, calculated as follows:

$$\frac{1}{N_{test}} \sum_{i=1}^{N_{test}} \frac{\mathbf{y}_i^\top (\mathbf{w}^*(\hat{\mathbf{y}}_i) - \mathbf{w}_i^*)}{\mathbf{y}_i^\top \mathbf{w}_i^*}. \quad (18)$$

where N_{test} is the number of test instances. Furthermore, each experiment is repeated five times with different seeds, and the average is

reported. The experiments were executed on an Intel i7-13800H (20 cores) CPU with 32GB RAM.

5.2 Experimental Results

5.2.1 Minimizing Surrogate Losses vs. Decision Losses with Differentiable Solver

In the first set of experiments, we investigate whether minimizing surrogate losses in the presence of differentiable optimization layers leads to lower regret compared to directly minimizing *Regret* or *SqDE*. We consider SP instances with gridsize 5 and 10; KP instances with 100 and 200 items, and CFL instances with 50 and 100 customers. In Figure 3a, Regret^{CVX} , SqDE^{CVX} , SPO_+^{CVX} , and SCE^{CVX} display the average test regret after minimizing *Regret*, *SqDE*, $\mathcal{L}_{\text{SPO}_+}$, and \mathcal{L}_{SCE} using Cvxpylayers as a differentiable solver, respectively. In Figure 3b, these losses are minimized using DYS-Net as the differentiable solver. Figures 3a and 3b show that minimizing \mathcal{L}_{SCE} or $\mathcal{L}_{\text{SPO}_+}$ consistently yields lower regret than minimizing *Regret* or *SqDE*, both when using an exact differentiable solver (Cvxpylayers) and an approximate one (DYS-Net).

5.2.2 Minimizing surrogate losses using different formulations.

The previous experiments showed that minimizing surrogate losses leads to lower test regret compared to directly minimizing regret using differentiable optimization. We now compare the quality and runtime of minimizing surrogate losses with different kinds of solvers. We will minimize both $\mathcal{L}_{\text{SPO}_+}$ and \mathcal{L}_{SCE} using two non-differentiable solvers – one solving the ILP formulation (for ILP problems) and one solving the LP relaxation; as well as two differentiable solvers: Cvxpylayers (an exact differentiable solver) and DYS-Net (an approximate, faster differentiable solver), which solve the ‘smoothed’ QP. In Figure 4, for SP, we do not consider the ILP formulation, as the LP formulation, itself, provides the exact solution.

In Figure 4a, minimizing $\mathcal{L}_{\text{SPO}_+}$ yields similar test regret regardless of the solver type. In contrast, minimizing \mathcal{L}_{SCE} with a non-differentiable solver leads to significantly higher regret, consistent with Theorem 2, which states that $\mathcal{L}_{\text{SPO}_+}$ is less sensitive to perturbations, while \mathcal{L}_{SCE} can result in non-zero regret from slight changes. As noted in Section 3.2, this issue with \mathcal{L}_{SCE} is mitigated by using a differentiable solver. Figure 4a confirms this: minimizing \mathcal{L}_{SCE} with a differentiable solver gives the lowest test regret, even lower compared to minimizing $\mathcal{L}_{\text{SPO}_+}$, whether $\mathcal{L}_{\text{SPO}_+}$ is minimized using a differentiable or non-differentiable solver. Figure 4b reports training times. DYS-Net is consistently faster. Thus, minimizing \mathcal{L}_{SCE} with DYS-Net achieves both low regret and low training time.

¹ Source code: <https://github.com/JayMan91/DYS-NET-SCE>.

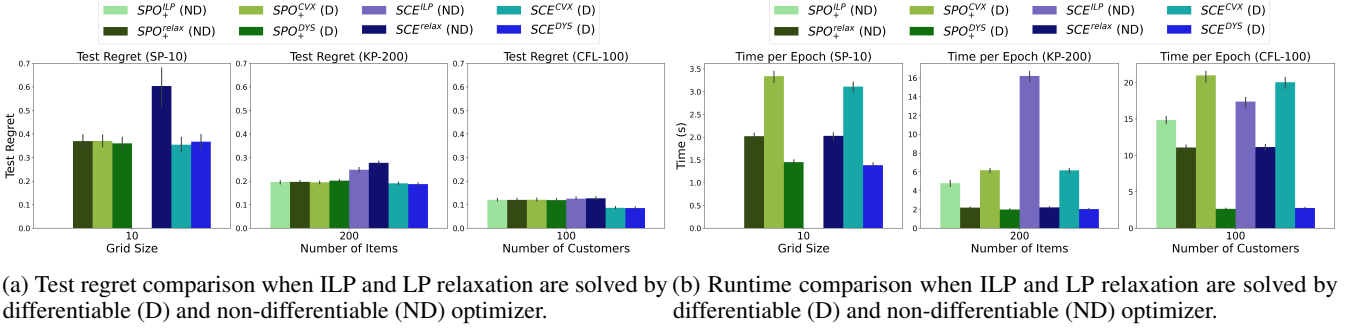


Figure 4: Minimizing surrogate losses using differentiable and non-differentiable optimizer.

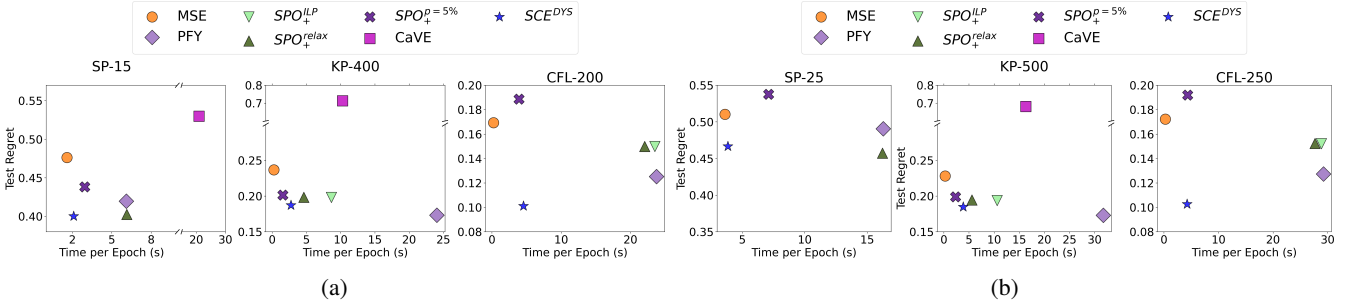


Figure 5: Comparison of Regret and Runtime against the state-of-the-art DFL techniques.

5.2.3 Comparison against the state of the art.

The previous experiments show that minimizing \mathcal{L}_{SCE} with a differentiable solver achieves regret comparable to minimizing \mathcal{L}_{SPO+} with a non-differentiable solver, one of the state-of-the-art DFL techniques. As DYS-Net is significantly faster than Cvxpylayers and the non-differentiable exact solvers, we propose minimizing \mathcal{L}_{SCE} using DYS-Net (SCE^{DYS}) to speed up DFL training without compromising quality. Hence in the final set of experiments, we compare the performance of SCE^{DYS} against ‘Perturbed Fenchel-Young’ (PFY) loss [5], the CaVE loss [31], SPO_+^{relax} and SPO_+^{ILP} , which minimize the \mathcal{L}_{SPO+} loss with and without LP relaxation, respectively, and the $SPO_+^{p=5\%}$ variant, which employs solution caching to solve (MI)LPs only 5% of the time [23].

We evaluate performance on larger problem instances: SP instances with gridsize 15 and 20; KP instances with 400 and 500 items, and CFL instances with 200 and 250 customers. In Figure 5, we plot the training time per epoch (x-axis) against normalized test regret (y-axis) to assess both solution quality and training efficiency. Minimizing MSE yields the lowest training time per epoch since no (MI)LPs are solved, but this often leads to higher test regret compared to DFL methods as it consider the downstream (MI)LPs while training

In the SP instances, SPO_+^{relax} achieves the lowest regret. The regret of SCE^{DYS} is second-lowest. Moreover, it requires only *one-third* the training time of SPO_+ . $SPO_+^{p=5\%}$ which solves the LP only 5% of times, is faster than SPO_+ but not as fast as SCE^{DYS} and its regret is also higher than SCE^{DYS} . For the KP instances, PFY achieves the lowest regret but it has the longest runtime. SCE^{DYS} is ranked second in terms of test regret – while being nearly five times faster than PFY. Although $SPO_+^{p=5\%}$ runs faster than SCE^{DYS} , its regret is slightly worse. SCE^{DYS} achieves both the *lowest runtime and the lowest regret* among the DFL techniques in the CFL instances. While $SPO_+^{p=5\%}$ has comparable runtime in these instances, its test regret is substantially higher than SCE^{DYS} . CaVE operates on active

constraints, which grow with problem size in SP and CFL. This makes CaVE memory-intensive, and we are unable to run it on all instances.

To summarize, SCE^{DYS} consistently matches or outperforms state-of-the-art DFL techniques, such as SPO_+ and PFY, in terms of regret, and significantly reduces training time across all problem instances – often by a factor of three or more compared to these methods. These results demonstrate that SCE^{DYS} achieves low regret with faster training times, making it an efficient choice for DFL involving (MI)LPs.

6 Conclusion

In this paper, we study the technique of making an (MI)LP differentiable by adding a quadratic regularizer to its objective. This technique is used in DFL to compute the Jacobian of the (MI)LP solution with respect to the cost parameters, and train an ML model to minimize regret by backpropagating through the smoothed QP. We first identify the zero-gradient issue exists even after smoothing for both small and large LPs through both numerical examples and simulations. To circumvent this issue, we propose minimizing a surrogate loss instead of the regret. We empirically show that minimizing the surrogate loss, \mathcal{L}_{SCE} , with a differentiable solver results in regret as low as or better than that of state-of-the-art surrogate-loss-based DFL techniques. Finally, by using DYS-Net, a fast approximate differentiable solver, to minimize \mathcal{L}_{SCE} , we demonstrate that DFL training time can be reduced by a factor of three without sacrificing decision regret.

A recent study [33] shows that the zero-gradient issue also occurs in problems with non-linear objectives. In future work, we plan to explore surrogate losses for such settings. Another direction for future work is to study ILPs with weaker LP relaxations, such as the MTZ formulation of the TSP [29], and examine how relying on the relaxation impacts decision quality when using DYS-Net. Future work could also explore alternative smoothing techniques or surrogate losses that could further improve the effectiveness of this approach.

Acknowledgements

This research received funding from the European Research Council (ERC) under the European Union’s Horizon 2020 research and innovation program (Grant No. 101002802, CHAT-Opt). Senne Berden is a fellow of the Research Foundation-Flanders (FWO-Vlaanderen, 11PQ024N).

References

- [1] A. Agrawal, B. Amos, S. Barratt, S. Boyd, S. Diamond, and J. Z. Kolter. Differentiable convex optimization layers. *Advances in neural information processing systems*, 32, 2019.
- [2] L. Alzubaidi, J. Zhang, A. J. Humaidi, A. Al-Dujaili, Y. Duan, O. Al-Shamma, J. Santamaría, M. A. Fadhel, M. Al-Amidie, and L. Farhan. Review of deep learning: concepts, cnn architectures, challenges, applications, future directions. *Journal of big Data*, 8:1–74, 2021.
- [3] B. Amos and J. Z. Kolter. Optnet: Differentiable optimization as a layer in neural networks. In *International Conference on Machine Learning*, pages 136–145. PMLR, 2017.
- [4] P. L. Bartlett and S. Mendelson. Rademacher and gaussian complexities: Risk bounds and structural results. *Journal of Machine Learning Research*, 3(Nov):463–482, 2002.
- [5] Q. Berthet, M. Blondel, O. Teboul, M. Cuturi, J.-P. Vert, and F. Bach. Learning with differentiable perturbed optimizers. *Advances in neural information processing systems*, 33:9508–9519, 2020.
- [6] M. Blondel, A. F. Martins, and V. Niculae. Learning with fenchel-young losses. *J. Mach. Learn. Res.*, 21(35):1–69, 2020.
- [7] S. Boyd and L. Vandenbergh. *Convex optimization*. Cambridge university press, 2004.
- [8] R. Cristian, P. Harsha, G. Perakis, B. L. Quanz, and I. Spantidakis. End-to-end learning for optimization via constraint-enforcing approximators. In *Proceedings of the AAAI Conference on Artificial Intelligence*, volume 37, pages 7253–7260, 2023.
- [9] D. Davis and W. Yin. A three-operator splitting scheme and its optimization applications. *Set-valued and variational analysis*, 25:829–858, 2017.
- [10] J. Duchi, S. Shalev-Shwartz, Y. Singer, and T. Chandra. Efficient projections onto the l_1 -ball for learning in high dimensions. In *Proceedings of the 25th International Conference on Machine Learning, ICML ’08*, page 272–279, New York, NY, USA, 2008. Association for Computing Machinery. ISBN 9781605582054. doi: 10.1145/1390156.1390191.
- [11] O. El Balghiti, A. N. Elmachtoub, P. Grigas, and A. Tewari. Generalization bounds in the predict-then-optimize framework. *Advances in neural information processing systems*, 32, 2019.
- [12] A. N. Elmachtoub and P. Grigas. Smart “predict, then optimize”. *Management Science*, 68(1):9–26, 2022.
- [13] A. Ferber, B. Wilder, B. Dilkina, and M. Tambe. Mipaal: Mixed integer program as a layer. *Proceedings of the AAAI Conference on Artificial Intelligence*, 34(02):1504–1511, Apr. 2020.
- [14] A. Ferber, E. Griffin, B. Dilkina, B. Keskin, and M. Gore. Predicting wildlife trafficking routes with differentiable shortest paths. In *Proceedings of the Integration of Constraint Programming, Artificial Intelligence, and Operations Research: 20th International Conference, CPAIOR 2023*, 2023.
- [15] S. W. Fung, H. Heaton, Q. Li, D. McKenzie, S. Osher, and W. Yin. Jfb: Jacobian-free backpropagation for implicit networks. In *Proceedings of the AAAI Conference on Artificial Intelligence*, volume 36, pages 6648–6656, 2022.
- [16] L. Gurobi Optimization. Gurobi optimizer reference manual. <http://www.gurobi.com>, 2021.
- [17] M. U. Gutmann and A. Hyvärinen. Noise-contrastive estimation of unnormalized statistical models, with applications to natural image statistics. *The journal of machine learning research*, 13(1):307–361, 2012.
- [18] J. Mandi and T. Guns. Interior point solving for lp-based prediction+optimisation. In H. Larochelle, M. Ranzato, R. Hadsell, M. Balcan, and H. Lin, editors, *Advances in Neural Information Processing Systems*, volume 33, pages 7272–7282, 2020.
- [19] J. Mandi, E. Demirović, P. J. Stuckey, and T. Guns. Smart predict-and-optimize for hard combinatorial optimization problems. *Proceedings of the AAAI Conference on Artificial Intelligence*, 34(02):1603–1610, Apr. 2020.
- [20] J. Mandi, V. Bucarey, M. M. K. Tchomba, and T. Guns. Decision-focused learning: Through the lens of learning to rank. In K. Chaudhuri, S. Jegelka, L. Song, C. Szepesvari, G. Niu, and S. Sabato, editors, *Proceedings of the 39th International Conference on Machine Learning*, volume 162 of *Proceedings of Machine Learning Research*, pages 14935–14947. PMLR, 17–23 Jul 2022.
- [21] J. Mandi, J. Kotary, S. Berden, M. Mulamba, V. Bucarey, T. Guns, and F. Fioretto. Decision-focused learning: Foundations, state of the art, benchmark and future opportunities. *Journal of Artificial Intelligence Research*, 80:1623–1701, 2024.
- [22] D. McKenzie, H. Heaton, and S. W. Fung. Differentiating through integer linear programs with quadratic regularization and davis-yin splitting. *Transactions on Machine Learning Research*, 2024. ISSN 2835-8856. URL <https://openreview.net/forum?id=H8IaxrANWl>.
- [23] M. Mulamba, J. Mandi, M. Diligenti, M. Lombardi, V. Bucarey, and T. Guns. Contrastive losses and solution caching for predict-and-optimize. In Z.-H. Zhou, editor, *Proceedings of the Thirtieth International Joint Conference on Artificial Intelligence, IJCAI-21*, pages 2833–2840. International Joint Conferences on Artificial Intelligence Organization, 8 2021. doi: 10.24963/ijcai.2021/390. Main Track.
- [24] M. Niepert, P. Minervini, and L. Franceschi. Implicit mle: Backpropagating through discrete exponential family distributions. In M. Ranzato, A. Beygelzimer, Y. Dauphin, P. Liang, and J. W. Vaughan, editors, *Advances in Neural Information Processing Systems*, volume 34, pages 14567–14579. Curran Associates, Inc., 2021.
- [25] A. Paszke, S. Gross, F. Massa, A. Lerer, J. Bradbury, G. Chanan, T. Killeen, Z. Lin, N. Gimelshein, L. Antiga, et al. Pytorch: An imperative style, high-performance deep learning library. *Advances in neural information processing systems*, 32, 2019.
- [26] M. V. Pogančić, A. Paulus, V. Musil, G. Martius, and M. Rolínek. Differentiation of blackbox combinatorial solvers. In *International Conference on Learning Representations*, 2020.
- [27] U. Sadana, A. Chenreddy, E. Delage, A. Forel, E. Frejinger, and T. Vidal. A survey of contextual optimization methods for decision-making under uncertainty. *European Journal of Operational Research*, 320(2):271–289, 2025. ISSN 0377-2217. doi: <https://doi.org/10.1016/j.ejor.2024.03.020>.
- [28] S. S. Sahoo, A. Paulus, M. Vlastelica, V. Musil, V. Kuleshov, and G. Martius. Backpropagation through combinatorial algorithms: Identity with projection works. In *The Eleventh International Conference on Learning Representations*, 2023.
- [29] H. D. Sherali and P. J. Driscoll. On tightening the relaxations of miller-tucker-zemlin formulations for asymmetric traveling salesman problems. *Operations Research*, 50(4):656–669, 2002.
- [30] B. Tang and E. B. Khalil. Pyepo: A pytorch-based end-to-end predict-then-optimize library for linear and integer programming, 2023.
- [31] B. Tang and E. B. Khalil. Cave: A cone-aligned approach for fast predict-then-optimize with binary linear programs. In B. Dilkina, editor, *Integration of Constraint Programming, Artificial Intelligence, and Operations Research - 21st International Conference, CPAIOR 2024, Uppsala, Sweden, May 28-31, 2024, Proceedings, Part II*, volume 14743 of *Lecture Notes in Computer Science*, pages 193–210. Springer, 2024.
- [32] V. Vapnik. Principles of risk minimization for learning theory. *Advances in neural information processing systems*, 4, 1991.
- [33] G. Vevurko, W. Böhmer, and M. de Weerd. You shall pass: Dealing with the zero-gradient problem in predict and optimize for convex optimization, 2024. URL <https://arxiv.org/abs/2307.16304>.
- [34] B. Wilder, B. Dilkina, and M. Tambe. Melding the data-decisions pipeline: Decision-focused learning for combinatorial optimization. In *The Thirty-Third AAAI Conference on Artificial Intelligence, AAAI 2019*, pages 1658–1665. AAAI Press, 2019.
- [35] L. A. Wolsey. *Integer Programming*. John Wiley & Sons, Ltd, 2020. ISBN 9781119606475.

A Predict-then-Optimize Problem Description

We consider predicting parameters in the objective function of an LP. These kinds of problems can be framed as *predict-then-optimize* (PtO) problems consisting of a prediction stage followed by an optimization stage, as illustrated in Figure 6. In the prediction stage, an ML model \mathcal{M}_θ (with trainable parameters ω) is used to predict unknown parameters using features, ψ , that are correlated to the parameter. During the optimization stage, the problem is solved with the predicted parameters. An offline dataset of past observations is available for training \mathcal{M}_θ .

It is important to distinguish datasets based on whether the true parameters, \mathbf{y} , are observed and included in the dataset. In some applications, the true parameters, \mathbf{y} , may not be directly observable, and only the solutions, $\mathbf{w}^*(\mathbf{y})$, are observed. While $\mathbf{w}^*(\mathbf{y})$ can be computed if \mathbf{y} is known, the reverse is not true, since solving the inverse optimization problem is a separate research area.

Whether \mathbf{y} is observed or not is important because in order to compute *Regret* (equation 3), we need the true parameter \mathbf{y} . Most of the benchmarks in PtO problems assume that \mathbf{y} is observed in the past observation. In this case the training data can be expressed as $\{(\psi_i, \mathbf{y}_i, \mathbf{w}^*(\mathbf{y}_i))\}_{i=1}^N$ and the empirical regret, $\frac{1}{N} \sum_{i=1}^N \text{Regret}(\mathbf{w}^*(\mathcal{M}_\theta(\psi_i)), \mathbf{y}_i)$, can be computed. In most PtO benchmark problems it is assumed that the true \mathbf{y} is observed in the training data [21, 30]. However, if the true cost \mathbf{y} is not observed in the training data, empirical regret cannot be computed. Instead, some other loss must be considered. For instance, McKenzie et al. [22] consider squared decision errors (SqDE) between $\mathbf{w}^*(\mathbf{y})$ and $\mathbf{w}^*(\hat{\mathbf{y}})$, i.e., $\text{SqDE} = \|\mathbf{w}^*(\mathbf{y}) - \mathbf{w}^*(\hat{\mathbf{y}})\|^2$.

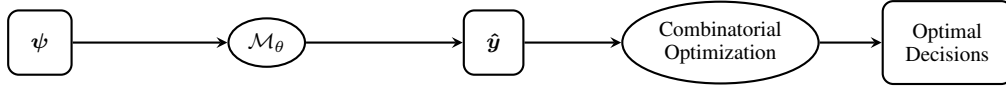


Figure 6: Schematic diagram of a predict-then-optimize (PtO) problem.

Algorithm 1 Gradient-descent with Smoothing

```

1: Initialize  $\omega$ .
2: for each epoch do
3:   for each instance  $(\psi, \mathbf{y}, \mathbf{w}^*(\mathbf{y}))$  do
4:      $\hat{\mathbf{y}} = \mathcal{M}_\theta(\psi)$ 
5:     Obtain  $\mathbf{w}^*(\hat{\mathbf{y}})$  by solving a ‘smoothed’ optimization
6:      $\text{Regret}(\mathbf{w}, \mathbf{y}) = \mathbf{y}^\top \mathbf{w}^*(\hat{\mathbf{y}}) - \mathbf{y}^\top \mathbf{w}^*(\mathbf{y})$ 
7:      $\omega \leftarrow \omega - \alpha \frac{d\text{Regret}(\mathbf{w}, \mathbf{y})}{d\hat{\mathbf{y}}} \frac{d\hat{\mathbf{y}}}{d\omega}$ 
8:   end for
9: end for
  
```

Algorithm 2 Gradient-descent with Surrogate Losses

```

1: for each epoch do
2:   for each instance  $(\psi, \mathbf{y}, \mathbf{w}^*(\mathbf{y}))$  do
3:      $\hat{\mathbf{y}} = \mathcal{M}_\theta(\psi)$ 
4:     Compute  $\tilde{\mathbf{y}}$ 
5:     Obtain  $\mathbf{w}^*(\tilde{\mathbf{y}})$  by solving the original optimization
6:     Compute the surrogate loss  $\mathcal{L}$  and  $\nabla$ 
7:      $\omega \leftarrow \omega - \alpha \nabla \frac{d\mathcal{L}}{d\tilde{\mathbf{y}}} \frac{d\tilde{\mathbf{y}}}{d\omega}$ 
8:   end for
9: end for
  
```

Algorithm 3 Gradient-descent when Surrogate Losses are minimized using Smoothed Solver

```

1: for each epoch do
2:   for each instance  $(\psi, \mathbf{y}, \mathbf{w}^*(\mathbf{y}))$  do
3:      $\hat{\mathbf{y}} = \mathcal{M}_\theta(\psi)$ 
4:     Compute  $\tilde{\mathbf{y}}$ 
5:     Obtain  $\mathbf{w}^*(\tilde{\mathbf{y}})$  by solving a ‘smoothed’ optimization
6:     Compute the surrogate loss  $\mathcal{L}$ 
7:      $\omega \leftarrow \omega - \alpha \frac{d\mathcal{L}}{d\hat{\mathbf{y}}} \frac{d\hat{\mathbf{y}}}{d\omega}$ 
8:   end for
9: end for
  
```

B Different Approaches to Decision-Focused Learning

In PtO problems, the empirical regret can be calculated if the cost, \mathbf{y} , is observed in the training instances. However, just because it can be calculated does not mean it can be minimized using gradient descent. Figure 8 illustrates the impact of integrating the optimization block into

the training loop of neural networks. The key challenge is that to directly minimize *Regret*, it must be backpropagated through the optimization problem. However, for a combinatorial problem $w^*(\hat{y})$ does not change smoothly with \hat{y} , so the gradient, $\frac{dw^*(\hat{y})}{d\hat{y}}$, is either zero or does not exist.



Figure 7: Schematic diagram showing the effect of QP smoothing. (a) LP solutions and the corresponding isocost line for four cost vectors. The green, cyan and red cost vectors result in the same solution, the top vertex, highlighting that a slight rotation of the isocost lines may not alter the LP solution. However, if the isocost lines rotate too much, for example, the violet line, the solution suddenly shifts to a different vertex. (b) The isocost lines change after applying QP smoothing, and the solution is no longer restricted to a vertex. For example, the red vector results in a smooth change in the solution. However, even with smoothing, some cost vectors, like the cyan and green, may still share the same solution.

Differentiable Optimization by Smoothing. ‘Differentiable Optimization by Smoothing’ is one approach to to circumvent this challenge. The aim of differentiable optimization is to represent an optimization problem as a differentiable mapping from its parameters to its solution. Since for a COP, this mapping is **not** differentiable, one prominent research direction in DFL involves smoothing the combinatorial optimization problem into a differentiable optimization problem. We particularly focus on smoothing by regularization. There exists another form of smoothing—smoothing by perturbation, as proposed by Pogančić et al. [26], Blondel et al. [6], Niepert et al. [24], Sahoo et al. [28]. In this work, we focus on optimization problems with linear objective functions such as LPs and ILPs. For an LP, the solution will always lie in one of the vertices of the LP simplex. So, the LP solution remains unchanged as long as the cost vector changes while staying within the corresponding normal cone [7]. However, the solution will suddenly switch to a different vertex if the cost vector slightly moves outside the normal cone, as illustrated in Figure 7a. Because the solution abruptly jumps between the vertices, the LP solution is not a differentiable function of the cost vector.

As explained in Section 2.1, approaches under this category replace the original optimization problem with a ‘smoothed’ version of the optimization problem, in which the solution can be expressed as a differentiable mapping of the parameter. For instance, if the original problem is an LP, it can be replaced with a QP by adding a quadratic regularizer to the objective of the LP.

The effect of QP smoothing is shown in Figure 7b. The arrows represent the cost vectors, while the nonlinear curves indicate the iso-cost curves. After smoothing, the solution is not restricted to being at a vertex of the LP polyhedron. In the ‘smoothed’ problem, unlike the original LP, the solution do not change abruptly. The solution either may not change or change smoothly with the change of the cost vector, as illustrated in Figure 7b. Consequently, $w^*(\hat{y})$ becomes differentiable with respect to \hat{y} and the solution, $w^*(y)$, can be represented as a differentiable function of the parameter y . When the problem is an ILP, first LP, resulting from continuous relaxation is considered and then it is smoothed by adding quadratic regularizer. Algorithm 1 explains this approach.

What we stress is that for a low smoothing strength (which ensures the solution after smoothing is not entire different from the LP solution), the QP solution might be same as the LP solution. Hence, two cost vectors can have the same solution. This is illustrated in Figure 7b. In this QP,

DYS-Net [22] provides an approximate solution to the quadratically regularized LP problem, where the computations are designed to be executed as standard neural network operations, enabling back-propagation through it. To summarize, approaches in this category follow the training loop in Figure 8 but only after ‘smoothing’ the optimization problem.

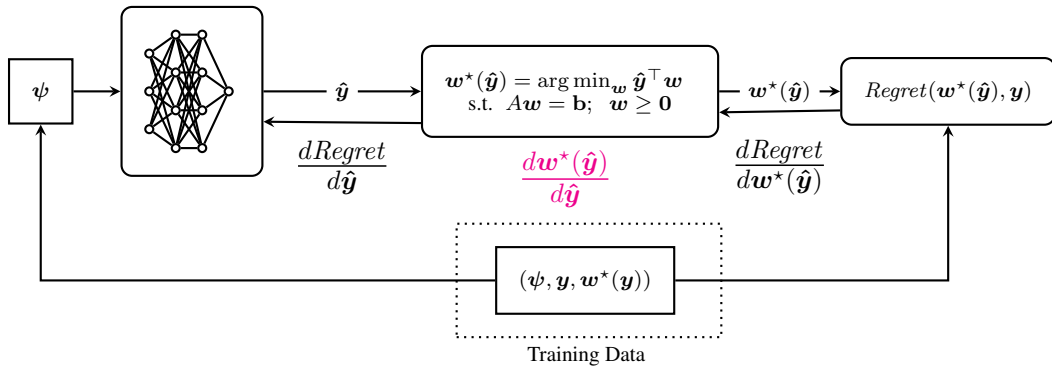


Figure 8: Decision-focused learning training loop.

Surrogate Losses for DFL. The primary goal of DFL is to minimize *Regret*. However, as explained earlier, *Regret* cannot be minimized directly due to its non-differentiability. Techniques involving surrogate losses aim to address this challenge by identifying suitable surrogate loss functions and computing gradients or subgradients of these surrogate losses for optimization. Figure 9 depicts the training loop of DFL using surrogate loss functions. In this approach, $\text{Regret}(\mathbf{w}^*(\hat{\mathbf{y}}), \mathbf{y})$ is not explicitly computed. Instead, after predicting $\hat{\mathbf{y}}$, a new cost vector $\tilde{\mathbf{y}}$ is generated based on $\hat{\mathbf{y}}$ and \mathbf{y} , and the optimization problem is solved using this $\tilde{\mathbf{y}}$. Subsequently, a surrogate loss is computed, using $\mathbf{w}^*(\tilde{\mathbf{y}})$ and $\mathbf{w}^*(\mathbf{y})$, and its gradient, ∇ (shown in pink), is used for backpropagation. We have explained this in terms of pseudocode using Algorithm 2. For example, in the case of $\mathcal{L}_{\text{SPO}+}$, $\tilde{\mathbf{y}} = 2\hat{\mathbf{y}} - \mathbf{y}$. As shown in Equation 5 $\mathcal{L}_{\text{SPO}+} = (2\hat{\mathbf{y}} - \mathbf{y})^\top \mathbf{w}^*(\mathbf{y}) - (2\hat{\mathbf{y}} - \mathbf{y})^\top \mathbf{w}^*(2\hat{\mathbf{y}} - \mathbf{y})$. Then the gradient used for backpropagation is $\nabla = 2(\mathbf{w}^*(\mathbf{y}) - \mathbf{w}^*(2\hat{\mathbf{y}} - \mathbf{y}))$. On the other hand, in the case of \mathcal{L}_{SCE} , $\tilde{\mathbf{y}} = \hat{\mathbf{y}}$ and $\mathcal{L}_{\text{SCE}} = \hat{\mathbf{y}}^\top (\mathbf{w}^*(\mathbf{y}) - \mathbf{w}^*(\hat{\mathbf{y}})) + \mathbf{y}^\top (\mathbf{w}^*(\hat{\mathbf{y}}) - \mathbf{w}^*(\mathbf{y}))$. So, in this case, the gradient for backpropagation is $\nabla = (\mathbf{w}^*(\mathbf{y}) - \mathbf{w}^*(\hat{\mathbf{y}}))$.

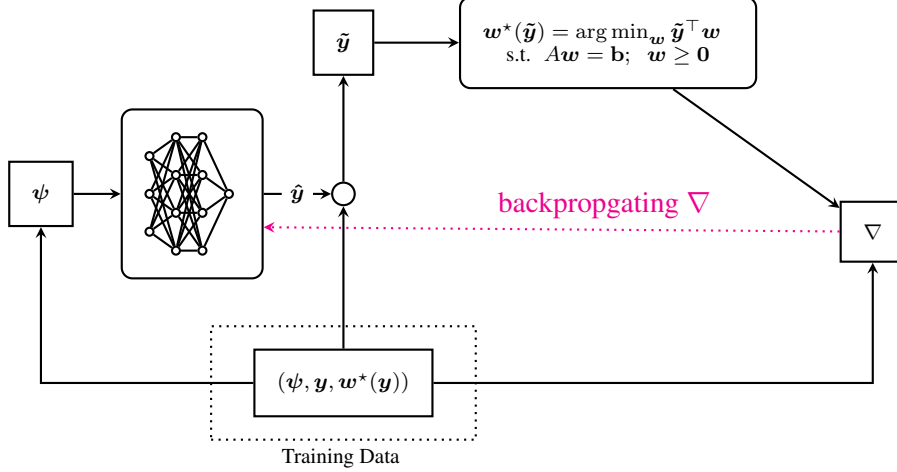


Figure 9: Decision-focused learning using surrogate loss functions.

Combining Surrogate Losses with Differentiable Optimization. The core idea proposed in this paper is to combine these two approaches. Specifically, the original optimization problem in Figure 9 is replaced with a smoothed version, **allowing direct backpropagation through the smoothed problem instead of using ∇** . We emphasize that this changes the gradient of the surrogate losses, i.e., Eq. 14 and Eq. 15 would reduce to SPO+ and SCE subgradients, respectively. We explain this in Algorithm 3.

C Proofs

C.1 Proof of Theorem 1

Proof. Let us consider the following optimization problem:

$$\min_{\mathbf{w} \in \mathcal{F}} \mathbf{y}^\top \mathbf{w}$$

We assume $\mathbf{w}^*(\mathbf{y})$ is the unique optimal solution, and therefore there is one unique $\mathbf{w}^*(\mathbf{y})$, so that, $\mathbf{w}'^\top \mathbf{y} - \mathbf{w}^*(\mathbf{y})^\top \mathbf{y} \geq 0 \forall \mathbf{w}' \in \mathcal{F}$. So, $\nabla_{\mathcal{L}_{\text{SPO}+}}$ would be zero only if the solution using $(2\hat{\mathbf{y}} - \mathbf{y})$ is same as the true solution $\mathbf{w}^*(\mathbf{y})$.

Hence we can write,

$$\begin{aligned} \nabla_{\mathcal{L}_{\text{SPO}+}} = 0 &\iff \mathbf{w}^*(2\hat{\mathbf{y}} - \mathbf{y}) = \mathbf{w}^*(\mathbf{y}) \iff (2\hat{\mathbf{y}} - \mathbf{y})^\top \mathbf{w}^*(\mathbf{y}) \leq (2\hat{\mathbf{y}} - \mathbf{y})^\top \mathbf{w}'; \forall \mathbf{w}' \in \mathcal{F} \\ &\iff 2\hat{\mathbf{y}}^\top (\mathbf{w}' - \mathbf{w}^*(\mathbf{y})) \geq \mathbf{y}^\top (\mathbf{w}' - \mathbf{w}^*(\mathbf{y})) \quad \forall \mathbf{w}' \in \mathcal{F} \\ &\iff \hat{\mathbf{y}}^\top \mathbf{w}' - \hat{\mathbf{y}}^\top \mathbf{w}^*(\mathbf{y}) \geq \frac{1}{2} \left(\mathbf{y}^\top (\mathbf{w}' - \mathbf{w}^*(\mathbf{y})) \right); \quad \forall \mathbf{w}' \in \mathcal{F} \end{aligned}$$

So, we can write:

$$\mathcal{Y}_{\text{SPO}+}(\mathbf{y}) = \{ \hat{\mathbf{y}} : \hat{\mathbf{y}}^\top \mathbf{w}' - \hat{\mathbf{y}}^\top \mathbf{w}^*(\mathbf{y}) \geq \frac{1}{2} \left(\mathbf{y}^\top (\mathbf{w}' - \mathbf{w}^*(\mathbf{y})) \right); \quad \forall \mathbf{w}' \in \mathcal{F} \} \quad (19)$$

As, $(\mathbf{y}^\top (\mathbf{w}' - \mathbf{w}^*(\mathbf{y}))) \geq 0$, we can write

$$\hat{\mathbf{y}}^\top \mathbf{w}' - \hat{\mathbf{y}}^\top \mathbf{w}^*(\mathbf{y}) \geq 0 \quad \forall \hat{\mathbf{y}} \in \mathcal{Y}_{\text{SPO}+}(\mathbf{y})$$

Hence, $\mathbf{w}^*(\mathbf{y})$ is an optimal solution to any $\hat{\mathbf{y}} \in \mathcal{Y}_{\text{SPO}+}(\mathbf{y})$.

Similarly, for \mathcal{L}_{SCE} ,

$$\begin{aligned} \nabla_{\mathcal{L}_{\text{SCE}}} = 0 &\iff \mathbf{w}^*(\hat{\mathbf{y}}) = \mathbf{w}^*(\mathbf{y}) \iff \hat{\mathbf{y}}^\top \mathbf{w}^*(\mathbf{y}) \leq \mathbf{y}^\top \mathbf{w}'; \quad \forall \mathbf{w}' \in \mathcal{F} \\ &\iff \hat{\mathbf{y}}^\top \mathbf{w}' - \hat{\mathbf{y}}^\top \mathbf{w}^*(\mathbf{y}) \geq 0; \quad \forall \mathbf{w}' \in \mathcal{F} \end{aligned}$$

Hence, we can write:

$$\mathcal{V}_{SCE}(\mathbf{y}) = \{\hat{\mathbf{y}} : \hat{\mathbf{y}}^\top \mathbf{w}' - \hat{\mathbf{y}}^\top \mathbf{w}^*(\mathbf{y}) \geq 0; \forall \mathbf{w}' \in \mathcal{F}\} \quad (20)$$

This shows that $\mathbf{w}^*(\mathbf{y})$ is an optimal solution to any $\hat{\mathbf{y}} \in \mathcal{V}_{SCE}(\mathbf{y})$. \square

C.2 Proof of Theorem 2

As a preliminary step toward the proof, we establish the following corollaries:

Corollary 3. For a given cost vector, $\mathbf{y} \in \mathbb{R}^K$, $\mathcal{V}_{SPO+}(\mathbf{y}) \subseteq \mathcal{V}_{SCE}(\mathbf{y})$.

Proof. We showed in equation 19 that

$$\mathcal{V}_{SPO+}(\mathbf{y}) = \{\hat{\mathbf{y}} : \hat{\mathbf{y}}^\top \mathbf{w}' - \hat{\mathbf{y}}^\top \mathbf{w}^*(\mathbf{y}) \geq \frac{1}{2}(\mathbf{y}^\top (\mathbf{w}' - \mathbf{w}^*(\mathbf{y})))\}; \forall \mathbf{w}' \in \mathcal{F}\}$$

We also proved in equation 20 that

$$\mathcal{V}_{SCE}(\mathbf{y}) = \{\hat{\mathbf{y}} : \hat{\mathbf{y}}^\top \mathbf{w}' - \hat{\mathbf{y}}^\top \mathbf{w}^*(\mathbf{y}) \geq 0; \forall \mathbf{w}' \in \mathcal{F}\}$$

As, $\mathbf{y}^\top (\mathbf{w}' - \mathbf{w}^*(\mathbf{y})) \geq 0$, it is clear that $\mathcal{V}_{SPO+}(\mathbf{y}) \subseteq \mathcal{V}_{SCE}(\mathbf{y})$. \square

Corollary 4. For a given $\mathbf{y} \in \mathbb{R}^K$, let us assume that there exists $\hat{\mathbf{y}}_1, \hat{\mathbf{y}}_2 \in \mathbb{R}^K$ and a feasible solution $\tilde{\mathbf{w}}$, such that

$$\hat{\mathbf{y}}_1^\top \tilde{\mathbf{w}} - \hat{\mathbf{y}}_1^\top \mathbf{w}^*(\mathbf{y}) \geq \frac{1}{2}(\mathbf{y}^\top (\tilde{\mathbf{w}} - \mathbf{w}^*(\mathbf{y})))$$

and

$$0 \leq \hat{\mathbf{y}}_2^\top \tilde{\mathbf{w}} - \hat{\mathbf{y}}_2^\top \mathbf{w}^*(\mathbf{y}) < \frac{1}{2}(\mathbf{y}^\top (\tilde{\mathbf{w}} - \mathbf{w}^*(\mathbf{y})))$$

Then the following statements hold:

1. If for any $\Delta \in \mathbb{R}^K$, $(\hat{\mathbf{y}}_1 + \Delta)^\top \mathbf{w}^*(\mathbf{y}) > (\hat{\mathbf{y}}_1 + \Delta)^\top \tilde{\mathbf{w}} \implies (\hat{\mathbf{y}}_2 + \Delta)^\top \mathbf{w}^*(\mathbf{y}) > (\hat{\mathbf{y}}_2 + \Delta)^\top \tilde{\mathbf{w}}$.
2. There exists $\Delta \in \mathbb{R}^K$, such that $(\hat{\mathbf{y}}_2 + \Delta)^\top \mathbf{w}^*(\mathbf{y}) > (\hat{\mathbf{y}}_2 + \Delta)^\top \tilde{\mathbf{w}}$, but $(\hat{\mathbf{y}}_1 + \Delta)^\top \mathbf{w}^*(\mathbf{y}) \leq (\hat{\mathbf{y}}_1 + \Delta)^\top \tilde{\mathbf{w}}$.

Proof. 1.

$$(\hat{\mathbf{y}}_1 + \Delta)^\top \mathbf{w}^*(\mathbf{y}) > (\hat{\mathbf{y}}_1 + \Delta)^\top \tilde{\mathbf{w}} \implies \Delta^\top (\mathbf{w}^*(\mathbf{y}) - \tilde{\mathbf{w}}) > \hat{\mathbf{y}}_1^\top (\tilde{\mathbf{w}} - \mathbf{w}^*(\mathbf{y})) \geq \frac{1}{2}\mathbf{y}^\top (\tilde{\mathbf{w}} - \mathbf{w}^*(\mathbf{y})) > \hat{\mathbf{y}}_2^\top (\tilde{\mathbf{w}} - \mathbf{w}^*(\mathbf{y}))$$

After rearranging, we can write:

$$(\hat{\mathbf{y}}_1 + \Delta)^\top \mathbf{w}^*(\mathbf{y}) > (\hat{\mathbf{y}}_1 + \Delta)^\top \tilde{\mathbf{w}} \implies (\hat{\mathbf{y}}_2 + \Delta)^\top \mathbf{w}^*(\mathbf{y}) > (\hat{\mathbf{y}}_2 + \Delta)^\top \tilde{\mathbf{w}}$$

2. We begin by writing the assumption

$$\hat{\mathbf{y}}_2^\top \tilde{\mathbf{w}} - \hat{\mathbf{y}}_2^\top \mathbf{w}^*(\mathbf{y}) < \frac{1}{2}(\mathbf{y}^\top (\tilde{\mathbf{w}} - \mathbf{w}^*(\mathbf{y})))$$

This implies the following:

$$\left(\hat{\mathbf{y}}_2 - \frac{1}{2}\mathbf{y}\right)^\top \tilde{\mathbf{w}} < \left(\hat{\mathbf{y}}_2 - \frac{1}{2}\mathbf{y}\right)^\top \mathbf{w}^*(\mathbf{y})$$

Be defining, $\Delta = -\frac{1}{2}\mathbf{y}$, we can write $(\hat{\mathbf{y}}_2 + \Delta)^\top \mathbf{w}^*(\mathbf{y}) > (\hat{\mathbf{y}}_2 + \Delta)^\top \tilde{\mathbf{w}}$.

But,

$$\hat{\mathbf{y}}_1^\top \tilde{\mathbf{w}} - \hat{\mathbf{y}}_1^\top \mathbf{w}^*(\mathbf{y}) \geq \frac{1}{2}(\mathbf{y}^\top (\tilde{\mathbf{w}} - \mathbf{w}^*(\mathbf{y})))$$

Hence, $(\hat{\mathbf{y}}_1 + \Delta)^\top \mathbf{w}^*(\mathbf{y}) \leq (\hat{\mathbf{y}}_1 + \Delta)^\top \tilde{\mathbf{w}}$. \square

Proof of Theorem 2.

Proof. We will use $\{\Delta\}_{SCE(\mathbf{y})}$ to denote the set of all Δ such that $(\hat{\mathbf{y}} + \Delta)^\top \mathbf{w}^*(\mathbf{y}) > (\hat{\mathbf{y}} + \Delta)^\top \mathbf{w}^*(\hat{\mathbf{y}} + \Delta)$ for any $\hat{\mathbf{y}} \in \mathcal{Y}_{SCE}(\mathbf{y})$. Similarly, $\{\Delta\}_{SPO+(\mathbf{y})}$ denotes the set of all Δ such that $(\hat{\mathbf{y}} + \Delta)^\top \mathbf{w}^*(\mathbf{y}) > (\hat{\mathbf{y}} + \Delta)^\top \mathbf{w}^*(\hat{\mathbf{y}} + \Delta)$ for any $\hat{\mathbf{y}} \in \mathcal{Y}_{SPO+}(\mathbf{y})$. This allows us to rewrite

$$\begin{aligned}\Gamma_{SCE} &= \min_{\Delta \in \{\Delta\}_{SCE(\mathbf{y})}} \|\Delta\|_2 \\ \Gamma_{SPO+} &= \min_{\Delta \in \{\Delta\}_{SPO+(\mathbf{y})}} \|\Delta\|_2\end{aligned}$$

We have proved in Corollary 3 that $\mathcal{Y}_{SPO+}(\mathbf{y}) \subseteq \mathcal{Y}_{SCE}(\mathbf{y})$. It is straightforward that if $\{\Delta\}_{SCE(\mathbf{y})}$ and $\{\Delta\}_{SPO+(\mathbf{y})}$ are the same set if $\mathcal{Y}_{SPO+}(\mathbf{y})$ and $\mathcal{Y}_{SCE}(\mathbf{y})$ are identical. Hence, in this case, it follows trivially that $\Gamma_{SCE} = \Gamma_{SPO+}$.

Let us consider the case, when $\mathcal{Y}_{SPO+}(\mathbf{y}) \subset \mathcal{Y}_{SCE}(\mathbf{y})$. This implies there exist a $\hat{\mathbf{y}}_2 \in \mathcal{Y}_{SCE}(\mathbf{y}) \setminus \mathcal{Y}_{SPO+}(\mathbf{y})$. The second statement in Corollary 4 shows that there exists a perturbation vector, Δ , such that $\mathbf{w}^*(\hat{\mathbf{y}}_2 + \Delta) \neq \mathbf{w}^*(\mathbf{y})$ for some $\hat{\mathbf{y}}_2 \in \mathcal{Y}_{SCE}(\mathbf{y}) \setminus \mathcal{Y}_{SPO+}(\mathbf{y})$, while for all $\hat{\mathbf{y}}_1 \in \mathcal{Y}_{SPO+}(\mathbf{y})$, $\mathbf{w}^*(\hat{\mathbf{y}}_1 + \Delta) = \mathbf{w}^*(\mathbf{y})$. Hence, $\Delta \in \{\Delta\}_{SCE(\mathbf{y})}$, but $\Delta \notin \{\Delta\}_{SPO+(\mathbf{y})}$.

Now, if for any $\hat{\mathbf{y}}_1 \in \mathcal{Y}_{SPO+}(\mathbf{y})$, $\mathbf{w}^*(\hat{\mathbf{y}}_1 + \Delta_1) \neq \mathbf{w}^*(\mathbf{y})$, then $\Delta_1 \in \{\Delta\}_{SPO+(\mathbf{y})}$. Moreover, as $\mathcal{Y}_{SPO+}(\mathbf{y}) \subset \mathcal{Y}_{SCE}(\mathbf{y})$, $\hat{\mathbf{y}}_1 \in \mathcal{Y}_{SCE}(\mathbf{y})$. Hence, $\Delta_1 \in \{\Delta\}_{SCE(\mathbf{y})}$. To summarize, $\Delta \in \{\Delta\}_{SPO+(\mathbf{y})} \implies \Delta \in \{\Delta\}_{SCE(\mathbf{y})}$, but not the reverse. So,

$$\{\Delta\}_{SPO+(\mathbf{y})} \subset \{\Delta\}_{SCE(\mathbf{y})}$$

As, $\{\Delta\}_{SPO+(\mathbf{y})} \subset \{\Delta\}_{SCE(\mathbf{y})}$,

$$\Gamma_{SPO+} = \min_{\Delta \in \{\Delta\}_{SPO+(\mathbf{y})}} \|\Delta\|_2 \geq \Gamma_{SCE} = \min_{\Delta \in \{\Delta\}_{SCE(\mathbf{y})}} \|\Delta\|_2$$

□

C.3 Proof of Proposition 1

Proof. 1. Following the definition of \mathcal{L}_{SCE} ,

$$\begin{aligned}\mathcal{L}_{SCE}(\mathbf{w}^*(\hat{\mathbf{y}}), \mathbf{y}) &= (\hat{\mathbf{y}} - \mathbf{y})^\top \mathbf{w}^*(\mathbf{y}) - (\hat{\mathbf{y}} - \mathbf{y})^\top \mathbf{w}^*(\hat{\mathbf{y}}) \\ &= \hat{\mathbf{y}}^\top (\mathbf{w}^*(\mathbf{y}) - \mathbf{w}^*(\hat{\mathbf{y}})) + \mathbf{y}^\top (\mathbf{w}^*(\hat{\mathbf{y}}) - \mathbf{w}^*(\mathbf{y}))\end{aligned}$$

- $\hat{\mathbf{y}}^\top (\mathbf{w}^*(\mathbf{y}) - \mathbf{w}^*(\hat{\mathbf{y}})) \geq 0$, because $\mathbf{w}^*(\hat{\mathbf{y}})$ is the optimal solution to $\hat{\mathbf{y}}$. In a similar way, $\mathbf{y}^\top (\mathbf{w}^*(\hat{\mathbf{y}}) - \mathbf{w}^*(\mathbf{y})) \geq 0$. Hence, $\mathcal{L}_{SCE}(\mathbf{w}^*(\hat{\mathbf{y}}), \mathbf{y}) \geq 0$.
2. We will prove the claim by contradiction. Assume that $\mathcal{L}_{SCE}(\mathbf{w}^*(\hat{\mathbf{y}}), \mathbf{y}) = 0$ but $\text{Regret}(\mathbf{w}^*(\hat{\mathbf{y}}), \mathbf{y}) = \mathbf{y}^\top (\mathbf{w}^*(\hat{\mathbf{y}}) - \mathbf{w}^*(\mathbf{y})) > 0$. This is possible if $\mathbf{w}^*(\hat{\mathbf{y}}) \neq \mathbf{w}^*(\mathbf{y})$. As the solution to $\hat{\mathbf{y}}$ is different from $\mathbf{w}^*(\mathbf{y})$, the singleton assumption implies that $\exists \mathbf{w}' \in \mathcal{F} \setminus \{\mathbf{w}^*(\mathbf{y})\} : \hat{\mathbf{y}}^\top \mathbf{w}' < \hat{\mathbf{y}}^\top \mathbf{w}^*(\mathbf{y})$. In this case, we have:

$$\begin{aligned}\hat{\mathbf{y}}^\top \mathbf{w}^*(\mathbf{y}) - \hat{\mathbf{y}}^\top \mathbf{w}' &> 0 \\ \implies (\hat{\mathbf{y}}^\top \mathbf{w}^*(\mathbf{y}) - \hat{\mathbf{y}}^\top \mathbf{w}') + (\mathbf{y}^\top \mathbf{w}' - \mathbf{y}^\top \mathbf{w}^*(\mathbf{y})) &> (\mathbf{y}^\top \mathbf{w}' - \mathbf{y}^\top \mathbf{w}^*(\mathbf{y})) \geq 0 \\ \implies (\hat{\mathbf{y}} - \mathbf{y})^\top \mathbf{w}^* - (\hat{\mathbf{y}} - \mathbf{y})^\top \mathbf{w}' &> 0\end{aligned}$$

In the second line, $\mathbf{y}^\top \mathbf{w}' - \mathbf{y}^\top \mathbf{w}^*(\mathbf{y})$ is added in both sides and this term is nonnegative as $\mathbf{w}^*(\mathbf{y})$ is the optimal solution to \mathbf{y} . This implies $\mathcal{L}_{SCE}(\mathbf{w}^*(\hat{\mathbf{y}}), \mathbf{y}) > 0$ and we arrive at a contradiction. Thus we prove that $\mathcal{L}_{SCE}(\mathbf{w}^*(\hat{\mathbf{y}}), \mathbf{y}) = 0 \implies \text{Regret}(\mathbf{w}^*(\hat{\mathbf{y}}), \mathbf{y}) = 0$.

Next, assume $\text{Regret}(\mathbf{w}^*(\hat{\mathbf{y}}), \mathbf{y}) = 0$. This implies that $\mathbf{y}^\top \mathbf{w}^*(\hat{\mathbf{y}}) = \mathbf{y}^\top \mathbf{w}^*(\mathbf{y})$. This can only be true if $\mathbf{w}^*(\hat{\mathbf{y}}) = \mathbf{w}^*(\mathbf{y})$ because of the singleton assumption. Hence, $\mathcal{L}_{SCE}(\mathbf{w}^*(\hat{\mathbf{y}}), \mathbf{y}) = (\hat{\mathbf{y}} - \mathbf{y})^\top (\mathbf{w}^*(\mathbf{y}) - \mathbf{w}^*(\hat{\mathbf{y}})) = 0$.

□

C.4 Generalization Bounds for SCE Loss

We show generalization bounds for SCE loss similar to the bounds shown for true regret by [11]. For notational brevity, we first define SCE in terms of the predicted and true parameters, i.e.,

$$l_{SCE}(\hat{\mathbf{y}}, \mathbf{y}) = \mathcal{L}_{SCE}(\mathbf{w}^*(\hat{\mathbf{y}}), \mathbf{y}) = (\hat{\mathbf{y}} - \mathbf{y})^\top (\mathbf{w}^* - \mathbf{w}^*(\hat{\mathbf{y}}))$$

where $\hat{\mathbf{y}} = \mathcal{M}(\psi)$ is the predicted cost using the predictive model \mathcal{M} . We can also define

$$R_{SCE}(\mathcal{M}) = \mathbb{E}[l_{SCE}(\mathcal{M}(\psi), \mathbf{y})] \text{ and } \hat{R}_{SCE}(\mathcal{M}) = \frac{1}{N} \sum_{i=1}^N l_{SCE}(\mathcal{M}(\psi_i), \mathbf{y}_i)$$

as the true and empirical risk for a given sample $\{(\psi_i, \mathbf{y}_i)\}_{i=1}^N$ for SCE loss, respectively.

In order to show generalization bounds for SCE loss, we need to define the Rademacher complexity of a set of functions \mathcal{H} with l_{SCE} . The sample Rademacher complexity for a given sample $\{(\psi_i, \mathbf{y}_i)\}_{i=1}^N$ is given by

$$\widehat{\mathfrak{R}}_{SCE}^N(\mathcal{H}) = \mathbb{E}_{\sigma} \left[\sup_{\mathcal{M} \in \mathcal{H}} \frac{1}{N} \sum_{i=1}^N \sigma_i l_{SCE}(\mathcal{M}(\psi_i), \mathbf{y}_i) \right]$$

where $\sigma_1, \sigma_2, \dots, \sigma_N$ are i.i.d. random variables with $\mathbb{P}(\sigma_i = 1) = 1/2$ and $\mathbb{P}(\sigma_i = -1) = 1/2$ for $i = 1, 2, \dots, N$. The expected Rademacher complexity is defined as $\mathfrak{R}_{SCE}^N(\mathcal{H}) = \mathbb{E}[\widehat{\mathfrak{R}}_{SCE}^N(\mathcal{H})]$ where the expectation is with respect to the i.i.d. samples of size N from the true distribution.

Assume that the set of all feasible solutions $\mathcal{F} = \{\mathbf{w} : A\mathbf{w} = \mathbf{b}; \mathbf{w} \geq \mathbf{0}\}$ is bounded, i.e., there exists D such that $D = \max_{\mathbf{w}, \mathbf{w}' \in \mathcal{F}} \|\mathbf{w} - \mathbf{w}'\|$. Also assume that the set of all cost vectors is \mathcal{Y} such that $\mathcal{Y} \subseteq \{\mathbf{y} : \|\mathbf{y}\| \leq 1\}$. Note that, since we consider linear objective functions, this assumption is not restrictive, as \mathbf{y}' with $\|\mathbf{y}'\| > 1$ can be replaced by $\mathbf{y} = \mathbf{y}'/\|\mathbf{y}'\|$ without changing the optimal solution and ensuring $\|\mathbf{y}\| = 1$.

The following proposition shows the generalization bound for SCE loss.

Proposition 2. *Let \mathcal{H} be a set of functions from the set of all features to $\{\mathbf{y} : \|\mathbf{y}\| \leq 1\}$. Then for any $\delta > 0$,*

$$R_{SCE}(\mathcal{M}) - \widehat{R}_{SCE}(\mathcal{M}) \leq 2\mathfrak{R}_{SCE}^N(\mathcal{H}) + 2D\sqrt{\frac{\log(1/\delta)}{2N}} \quad (21)$$

holds for all $\mathcal{M} \in \mathcal{H}$ with probability at least $1 - \delta$ for the sample $\{(\psi_i, \mathbf{y}_i)\}_{i=1}^N$ from the joint distribution of features and parameters. If $\widehat{\mathcal{M}}_n$ is a minimizer of the empirical risk \widehat{R}_{SCE} , then the inequality

$$R_{SCE}(\widehat{\mathcal{M}}_n) - \min_{\mathcal{M} \in \mathcal{H}} R_{SCE}(\mathcal{M}) \leq 2\mathfrak{R}_{SCE}^N(\mathcal{H}) + 4D\sqrt{\frac{\log(2/\delta)}{2N}} \quad (22)$$

also holds probability at least $1 - \delta$.

Proof. The SCE loss is bounded for all $\mathbf{y}, \mathbf{y}' \in \mathcal{Y}$ since $l_{SCE}(\hat{\mathbf{y}}, \mathbf{y}) = (\hat{\mathbf{y}} - \mathbf{y})^\top (\mathbf{w}^* - \mathbf{w}^*(\hat{\mathbf{y}})) \leq \|\hat{\mathbf{y}} - \mathbf{y}\| \|\mathbf{w}^* - \mathbf{w}^*(\hat{\mathbf{y}})\| \leq 2D$ where the first inequality is due to Cauchy–Schwarz and the second inequality is due to our assumptions on the hypothesis class and the feasible region. Then, inequality 21 follows directly from the classical generalization bound as shown in [4].

The extension of inequality 21 to inequality 22 is shown in the proof of Corollary 1 in [11] using Hoeffding’s inequality. \square

D Computational Experiments Demonstrating Zero Gradient

In Section 3, we made the case for minimizing surrogate loss such as \mathcal{L}_{SCE} instead of *Regret*. Our main argument is for a relatively low value of smoothing parameter μ , *Regret* will have zero gradient. However, \mathcal{L}_{SCE} will not have this problem. We provided two illustrations considering small-scale optimization problems. Here, we justify this with higher-dimensional optimization problems. We consider Top-1 selection problem with different number of items M .

$$\max_{\mathbf{w} \in \{0,1\}} \mathbf{y}^\top \mathbf{w} \text{ s.t. } \mathbf{w}^\top \mathbf{1} \leq 1 \quad (23)$$

$\mathbf{y} = [y_1, \dots, y_M] \in \mathbb{R}^M$ is the vector denoting value of all the items and $\mathbf{w} = [w_1, \dots, w_M]$ is the vector decision variables. To replicate the setup of a PtO problem, we solve the optimization problem with $\hat{\mathbf{y}}$. Let us assume $y_i, \hat{y}_i \geq 0$.

Before, solving the problem with simulation, we will show one interesting aspect of this problem. Note that when $\mu > 0$, the following relaxed optimization problem is solved:

$$\max_{\mathbf{w}} \mathbf{y}^\top \mathbf{w} - \frac{\mu}{2} \|\mathbf{w}\|^2 \text{ s.t. } \mathbf{w}^\top \mathbf{1} \leq 1; \mathbf{w} \geq \mathbf{0} \quad (24)$$

We point out that the solution to the unconstrained optimization problem is $v_i^* = \frac{y_i}{\mu} > 0$.

The augmented Lagrangian of Equation 24 is

$$\mathbb{L} = \mathbf{y}^\top \mathbf{w} - \frac{\mu}{2} \|\mathbf{w}\|^2 + \lambda(1 - \mathbf{w}^\top \mathbf{1}) + \boldsymbol{\sigma}^\top \mathbf{w} \quad (25)$$

where λ and $\boldsymbol{\sigma} = [\sigma_1, \dots, \sigma_M]$ are dual variables. By differentiating \mathbb{L} with respect to v_i , we obtain one condition of optimality, which is the following:

$$y_i - \mu v_i - \lambda + \sigma_i = 0 \implies v_i = \frac{y_i - \lambda + \sigma_i}{\mu} \quad (26)$$

Without any loss of generality, let $y^{(1)} \geq y^{(2)} \geq \dots y^{(M)}$. (In the d) As, solution to the constrained optimization problem is $v_i > 0$, $y^{(1)}$ will definitely be greater than zero. Hence, $\sigma_i = 0$ because of strict complementarity. So, we can write $v^{(1)} - v^{(k)} = \frac{y^{(1)} - y^{(k)} - \sigma^{(k)}}{\mu}$. As, $v^{(1)} - v^{(k)} \leq 1$, we can write:

$$\frac{y^{(1)} - y^{(k)} - \sigma^{(k)}}{\mu} \leq 1 \implies \mu \geq y^{(1)} - y^{(k)} - \sigma^{(k)} \quad (27)$$

So,

$$y^{(1)} - y^{(k)} > \mu \implies \sigma^{(k)} > 0 \implies y^{(k)} = 0 \quad (28)$$

This suggest that if $y^{(k)} < y^{(1)} - \mu$, only $v^{(1)} = 1$ and all other decision variables will be zero in the optimal solution.

To generate the ground truth \mathbf{y} , we randomly select M integers without replacement from the set $1, \dots, M$. The predicted costs, $\hat{\mathbf{y}}$, are generated by considering a different sample from the same set. As a result, \mathbf{y} and $\hat{\mathbf{y}}$ contain the same numbers but in different permutations. It is important to note that all elements in both vectors are positive integer values. We compute the solution to the optimization problem for \mathbf{y} and $\hat{\mathbf{y}}$. We solve the optimization problem with $\hat{\mathbf{y}}$ using a ‘smoothed’ optimization layer—*CvxpyLayer*. In order to compare the gradients of *Regret* and \mathcal{L}_{SCE} . We compute the gradients of both the losses for multiple values of M and μ . For each configuration of M and μ , we run 20 simulations.

μ	M					
	5	10	20	40	80	100
0.100	0.000	0.000	0.000	0.000	0.000	0.000
0.500	0.000	0.000	0.000	0.000	0.000	0.000
0.990	0.000	0.000	0.000	0.000	0.000	0.001
1.050	0.089	0.089	0.089	0.089	0.089	0.089
1.500	0.465	0.466	0.465	0.465	0.465	0.464
2.000	0.622	0.622	0.622	0.622	0.622	0.622
5.000	1.165	1.165	1.165	1.165	1.165	1.165

Table 2: We tabulate average Manhattan distance between the solution of the ‘smoothed’ problem and the solution of the original problem for different values of M and μ .

Note that $y^{(1)} > y^{(2)} > \dots y^{(M)}$ because of the way we created the dataset. Moreover, as all values in $\hat{\mathbf{y}}$ and \mathbf{y} are integer, Equation 28 suggests if $\mu < 1$, the solution to the relaxed problem (equation 24) will be binary. So, the discussion in Section 3 suggests that slight change of the cost parameter would not change the solution and hence the zero gradient problem would appear while differentiating *Regret*.

In Figure 10, we plotted the average absolute values of the gradients of the two losses— \mathcal{L}_{SCE} and *Regret*. As we hypothesized the gradient turns zero whenever *Regret* is minimized with $\mu < 1$. It is true that for $\mu > 1$, *Regret* have non-zero gradient. However, higher values of μ turns solution to the ‘smoothed’ problem very different from the solution to the original problem. We show this in Table 2 by displaying the average Manhattan distance between solutions of the true and ‘smoothed’ problem for same $\hat{\mathbf{y}}$.

We also highlight that, for the same values of μ , the average Manhattan distances remain same across different M . Examining the results of the simulations, we observed that the solution to the smoothed problem is fractional. For example, when $\mu = 2$, the solution includes two non-zero values—0.77 and 0.23. Typically, the value 0.77 appears in the position corresponding to the highest value in $\hat{\mathbf{y}}$, i.e., where there is a 1 in solution vector. As a result, the Manhattan distance becomes $(1-0.77)+0.23 = 0.46$. Interestingly, these values remain unchanged across different values of M . Therefore, the Manhattan distance remains constant as long as μ does not change.

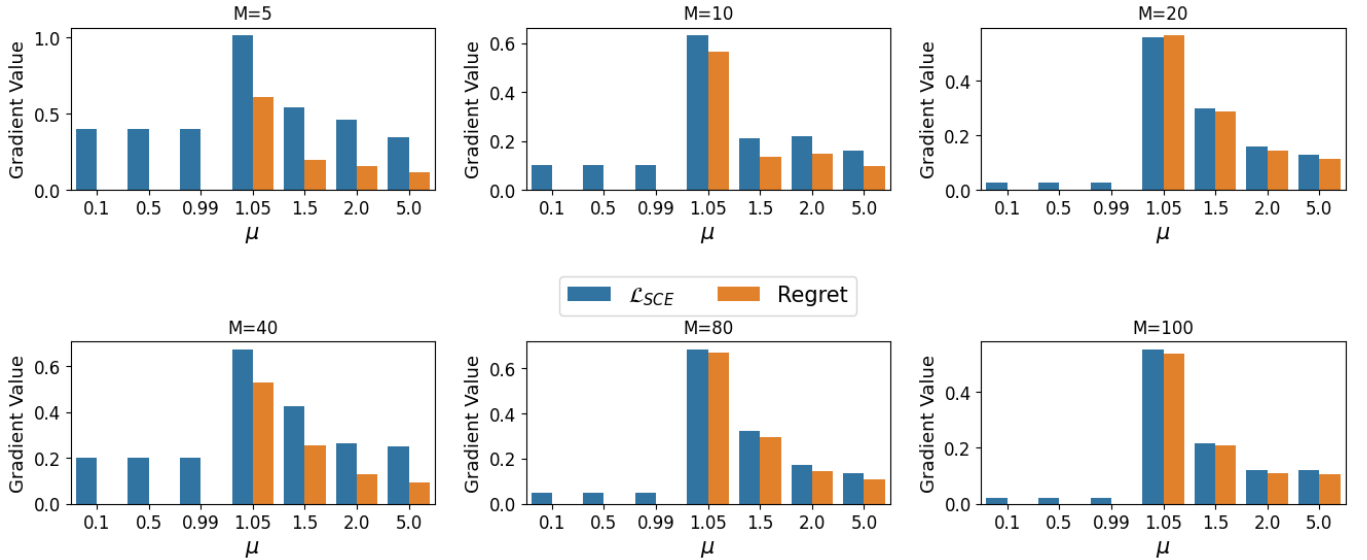


Figure 10: Results of Computational Simulation

E Demonstration of Learning with \mathcal{L}_{SCE} versus Regret

We further illustrate this with a simple fractional knapsack problem, which is an LP. Let us consider that we have two items and space for only one item. This can be formulated as a minimization problem:

$$\min -y_1 v_1 - y_2 v_2 \quad \text{s.t.} \quad v_1 + v_2 \leq 1; \quad v_1, v_2 \geq 0$$

Let us assume the true values of y_1 and y_2 are $(0.8, 0.4)$. The corresponding solution is $(v_1, v_2) = (1, 0)$. The grey region in Figure 11 corresponds to any predictions satisfying $\hat{y}_1 > \hat{y}_2$. Such predictions will induce the true solution, resulting in zero regret. Further assume that the initial predictions are $(\hat{y}_1, \hat{y}_2) = (0.1, 0.01)$. We show the progression of predictions by epochs when regret and SCE are used as training loss, using the smoothed optimization problem with blue and green lines, respectively in Figure 11. The predictions does not change with training epochs when regret is used as the loss because the derivatives of regret with respect to \hat{y}_1 and \hat{y}_2 are zero. On the other hand, when \mathcal{L}_{SCE} is used as the loss, (\hat{y}_1, \hat{y}_2) gradually move from the white region to the grey region, eventually resulting in zero regret. Note that increasing the strength of smoothing may provide non-zero gradient across the space. But this will entirely alter the optimization problem's solution. For instance, in this knapsack example, high values of μ would make both v_1 and v_2 close to zero.

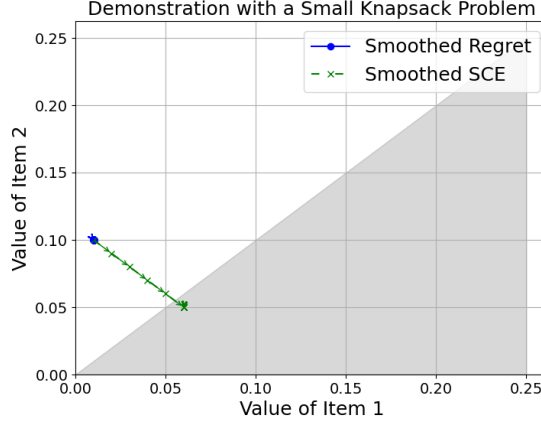


Figure 11: Progression of predictions by epochs when the smoothed regret and SCE are used as training losses.

F Description of The Optimization Problem and Data Generation Process

In this section, we first describe the optimization problems along with their formulations, followed by details of the data generation process and the ML models.

F.1 Description of the Optimization Problems

Shortest Path Problem. It is a shortest path problem on a $k \times k$ grid, with the objective of going from the southwest corner of the grid to the northeast corner where the edges can go either north or east. This grid consists of k^2 nodes and $2 \times k \times (k - 1)$ edges. Let, y_{ij} is the cost of going from node i to node j and the decision variable w_{ij} takes the value 1 if and only if the edge from node i to node j is traversed. Then, the shortest path problem from going to node s to node t can be formulated as an LP problem in the following form:

$$\min_{w_{ij}} \sum_{(i,j) \in \mathcal{E}} y_{ij} w_{ij} \quad (29a)$$

s.t.

$$\sum_{(i,j) \in \mathcal{E}} w_{ij} - \sum_{(k,i) \in \mathcal{E}} w_{ki} = \begin{cases} 1 & \text{if } i = s \\ -1 & \text{if } i = t \\ 0 & \text{otherwise} \end{cases} \quad (29b)$$

$$w_{ij} \in \mathbb{R}^+ \quad (29c)$$

Knapsack Problem. In a knapsack problem the goal of the optimization problem is to choose a maximal value subset from a given set of items, subject to some capacity constraints. Let the set contains N_{items} number of items and the value of each item is y_i . The solution must satisfy capacity constraints in multiple dimensions. Let C_j is the capacity in dimension j and $\phi_{(i,j)}$ is the weight of item i in dimension j . This optimization can be modeled as an integer linear programming (ILP) as follows:

$$\min_{w_1, \dots, w_{N_{items}}} \sum_{i=1}^{N_{items}} (-y_i) w_i \quad (30a)$$

s.t.

$$\sum_{i=1}^{N_{items}} \phi_{(i,j)} w_i \leq C_j ; \forall j \quad (30b)$$

$$w_i \in \{0, 1\} \quad (30c)$$

The Top-K selection can be viewed as a special case of the knapsack problem. In the Top-K, there is only one dimension and the weight of each item is 1 and the capacity, $C = K$.

Capacitated facility location problem. Provided a set of locations for opening facilities, F , and a set of customers, C , the objective is to minimize the total operation cost while satisfying the customer demands of a single product. Each customer $c \in C$ has a demand D_c , and each facility $f \in F$ has a capacity Cap_f and incurs a fixed opening cost FC_f . A transportation cost is incurred to serve customer c from facility f . The two constraints are to ensure that each customer's demand is fully met and ensuring the total demand assigned to a facility does not exceed its capacity. The decision variables are:

- $w_{c,f} \in [0, 1]$: the fraction of client c 's demand assigned to facility f ,
- $W_f \in \{0, 1\}$: a binary variable indicating whether facility f is open.

It is an MILP, as it has both integer and continuous variables. The formulation of the problem is the following:

$$\min_{w_{c,f}, W_f} \sum_{c \in C} \sum_{f \in F} w_{c,f} y_{c,f} D_c + \sum_{f \in F} \text{FC}_f \cdot W_f \quad (31a)$$

$$\text{s.t.} \quad \sum_{f \in F} w_{c,f} = 1, \quad \forall c \in C, \quad (31b)$$

$$\sum_{c \in C} D_c \cdot w_{c,f} \leq \text{Cap}_f \cdot W_f, \quad \forall f \in F, \quad (31c)$$

$$w_{c,f} \geq 0, \quad W_f \in \{0, 1\}, \quad \forall c \in C, \forall f \in F. \quad (31d)$$

In the PtO version, the transportation costs are unknown, all other parameters are known.

F.2 Description of the Data Generation Process

We use PyEPO library [30] to generate training, validation and test datasets. Each dataset consists of $\{(\psi_i, \mathbf{y}_i)\}_{i=1}^N$, which are generated synthetically. The feature vectors are sampled from a multivariate Gaussian distribution with zero mean and unit variance, i.e., $\psi_i \sim \mathbf{N}(0, I_p)$, where p is the dimension of ψ_i . To generate the cost vector, first a matrix $B \in \mathbb{R}^{K \times p}$ is generated, which represents the true underlying model, unknown to the modeler. Each element in the cost vector $y_{i,j}$ is then generated according to the following formula:

$$\mathbf{y}_{ij} = \left[\frac{1}{3 \cdot 5^{\text{Deg}}} \left(\frac{1}{\sqrt{p}} (B\psi_i) + 3 \right)^{\text{Deg}} + 1 \right] \xi_i^j \quad (32)$$

The Deg is 'model misspecification' parameter. This is because a linear model is used as a predictive model in the experiment and a higher value of Deg indicates the predictive model deviates more from the true underlying model and larger the prediction errors. ξ_i^j is a multiplicative noise term sampled randomly from the uniform distribution $\xi_i^j \sim U[1 - w, 1 + w]$. w is a noise-half width parameter, which is less than 1. Higher values of w indicate a greater degree of noise perturbation. We set Deg to 6 and w to 0.5 in all our experiments.

G Retrieving only the Active Constraints on the Knapsack Problem

Consider the two-dimensional knapsack example in Figure 12. The capacity constraint is given as $3v_1 + 3v_2 \leq 5$. If the objective vector \mathbf{y} lies within the union of the yellow and red cones, then the feasible solution (1,0) is optimal for the problem with the integrality constraint. So, the true normal cone is the union of the yellow and red cones. Note that the constraint $3v_1 + 3v_2 \leq 5$ is not active, although it plays a key role in choosing the solution; in the absence of this constraint, the solution would be (1, 1). In this case, the only active constraints are $v_1 = 1$ and $v_2 = 0$. As the CaVE approach stores only these two constraints, the yellow cone is considered as the optimality cone. This example shows that the mismatch between the cone of optimality of the integer knapsack and its relaxation can be non-trivial (the red cone in Figure 12). This attributes to the poor performance of the CaVE approach in the Knapsack problem.

H Experimental Details

H.1 Hyperparameter

We tuned all hyperparameters on the validation set and found that a learning rate of 0.005 consistently yielded the lowest validation regret across all problems. Since the mapping between \mathbf{y} and ψ follows the same data generation process in every case, we adopted this learning rate for all experiments. Additionally, PFY includes an extra hyperparameter: the temperature parameter. After tuning, based on validation regret, we set the following values of the temperature parameter.

Problem	Temperature parameter value
SP	1.
KP	1.
CFL	1.

Table 3: Value of Temperature Hyperparameter of the PFY Method

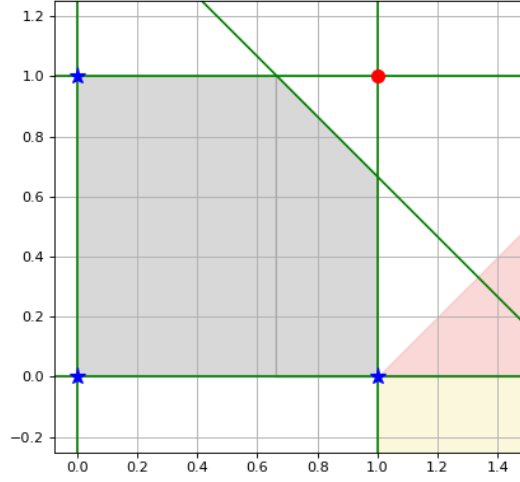


Figure 12: A numerical illustration to show why the approach of retrieving active constraints does not work in the Knapsack problems.

H.2 Implementation of DYS

We adopt the implementation by McKenzie et al. [22] to implement DYS-Net². DYS-Net includes a few hyperparameters: μ , controls the strength of smoothing; scaling parameter $\alpha \in (0, 2/\mu)$; number of time Equation 4 is iterated. (For detailed explanations of these parameters, please refer to the original papers.) In practice, we set the number of iterations to 100, because this results in good quality performances across all instances. We agree it might be possible to tune to specific problems to achieve even faster implementation without compromising performance. Each iteration is implemented as a multi-layer perceptron (MLP), making the implementation computationally efficient. We tune the parameter α on a validation set. In most cases, we keep it low ≈ 0.01 . Notably, DYS-Net implementation does not require pretraining, as DYS-Net contains no trainable parameters.

H.3 DYS-Net Hyperparameter

Problem	α	τ
SP-5	0.01	0.
SP-10	0.01	1.
SP-15	0.01	0.
SP-25	0.01	0.
KP-100	0.01	1.
KP-200	0.01	0.
KP-400	0.01	0.
KP-500	0.01	0.
CFL-50	0.01	0.1
CFL-100	0.01	0.1
CFL-200	0.01	0.1
CFL-250	0.01	0.1

Table 4: Value of SCE^{DYS} Hyperparameters

² <https://github.com/mines-opt-ml/fpo-dys>

H.4 Tabular Result

Gridsize	Model	Normalized Regret	Runtime (sec.)
5	$Regret^{CVX}$	0.36	3.66
	$Regret^{DYS}$	0.35	0.93
	SCE^{CVX}	0.31	3.67
	SCE^{DYS}	0.32	0.94
	SPO^{CVX}	0.32	3.13
	SPO^{DYS}	0.33	0.92
	SPO^{relax}	0.32	0.73
	$SqDE^{CVX}$	0.36	3.71
	$SqDE^{DYS}$	0.34	0.73
	CaVE	0.33	3.42
	MSE	0.45	0.26
	PFY	0.32	0.73
10	$Regret^{CVX}$	0.45	3.25
	$Regret^{DYS}$	0.41	1.63
	SCE^{CVX}	0.35	3.24
	SCE^{DYS}	0.37	1.44
	SPO^{CVX}	0.37	3.48
	SPO^{DYS}	0.36	1.51
	SPO^{relax}	0.37	2.10
	$SqDE^{CVX}$	0.52	3.31
	$SqDE^{DYS}$	0.41	1.56
	CaVE	0.48	11.89
	MSE	0.46	0.26
	PFY	0.37	2.12
15	$Regret^{DYS}$	0.44	2.08
	SCE^{DYS}	0.40	2.10
	SPO^{DYS}	0.39	2.09
	$SPO^{p=5\%}$	0.44	2.94
	SPO^{relax}	0.40	6.15
	$SqDE^{DYS}$	0.47	2.04
	CaVE	0.53	20.93
	MSE	0.48	1.58
	PFY	0.42	6.12
25	$Regret^{DYS}$	0.48	3.85
	SCE^{DYS}	0.47	3.85
	SPO^{DYS}	0.45	3.77
	$SPO^{p=5\%}$	0.54	7.10
	SPO^{relax}	0.46	16.22
	$SqDE^{DYS}$	0.58	3.70
	MSE	0.51	3.62
	PFY	0.49	16.29

Table 5: Result on Shortest Path Instances

numitems	Model	Normalized Regret	Runtime (sec.)
100	$Regret^{CVX}$	0.30	6.00
	$Regret^{DYS}$	0.22	1.59
	SCE^{CVX}	0.18	5.97
	SCE^{DYS}	0.18	1.48
	SPO^{CVX}	0.19	5.78
	SPO^{DYS}	0.20	1.55
	SPO_{+}^{LP}	0.20	2.29
	SPO_{+}^{relax}	0.20	1.31
	$SqDE^{CVX}$	0.24	5.96
	$SqDE^{DYS}$	0.18	1.55
	CaVE	0.76	8.64
	MSE	0.23	0.33
	PFY	0.18	5.97
200	$Regret^{CVX}$	0.32	6.38
	$Regret^{DYS}$	0.24	1.98
	SCE^{CVX}	0.19	6.41
	SCE^{DYS}	0.19	2.11
	SPO^{CVX}	0.19	6.42
	SPO^{DYS}	0.20	2.06
	SPO_{+}^{LP}	0.20	4.98
	SPO_{+}^{relax}	0.20	2.28
	$SqDE^{CVX}$	0.31	6.40
	$SqDE^{DYS}$	0.20	1.93
	CaVE	0.76	9.62
	MSE	0.24	0.34
	PFY	0.18	12.97
400	$Regret^{DYS}$	0.25	2.65
	SCE^{DYS}	0.19	2.76
	SPO^{DYS}	0.21	2.72
	SPO_{+}^{LP}	0.20	8.65
	$SPO_{+}^{p=5\%}$	0.20	1.56
	SPO_{+}^{relax}	0.20	4.63
	$SqDE^{DYS}$	0.20	2.46
	CaVE	0.71	10.28
	MSE	0.24	0.26
	PFY	0.17	24.05
500	$Regret^{DYS}$	0.24	3.85
	SCE^{DYS}	0.18	3.86
	SPO^{DYS}	0.20	3.81
	SPO_{+}^{LP}	0.19	10.60
	$SPO_{+}^{p=5\%}$	0.20	2.33
	SPO_{+}^{relax}	0.19	5.60
	$SqDE^{DYS}$	0.20	3.87
	CaVE	0.68	16.30
	MSE	0.23	0.27
	PFY	0.17	31.73

Table 6: Result on Knapsack Instances

No. of Customers	No. of Facilities	Model	Normalized Regret	Runtime (sec.)
50	5	$Regret^{CVX}$	0.22	8.01
		$Regret^{DYS}$	0.09	1.65
		SCE^{CVX}	0.09	8.03
		SCE^{DYS}	0.08	1.72
		SPO^{CVX}	0.09	7.23
		SPO^{DYS}	0.09	1.58
		SPO^{ILP}	0.09	4.94
		SPO^{relax}	0.09	3.31
		$SqDE^{CVX}$	0.19	8.02
		$SqDE^{DYS}$	0.09	1.62
		CaVE	0.11	12.19
		MSE	0.11	0.34
		PFY	0.08	4.98
100	10	$Regret^{CVX}$	0.20	20.48
		$Regret^{DYS}$	0.18	2.99
		SCE^{CVX}	0.09	20.88
		SCE^{DYS}	0.09	2.89
		SPO^{CVX}	0.12	21.85
		SPO^{DYS}	0.12	2.76
		SPO^{ILP}	0.12	15.47
		SPO^{relax}	0.12	11.53
		$SqDE^{CVX}$	0.11	19.38
		$SqDE^{DYS}$	0.12	2.79
		CaVE	0.12	34.83
		MSE	0.14	0.38
		PFY	0.10	16.66
200	10	$Regret^{DYS}$	0.25	4.62
		SCE^{DYS}	0.10	4.55
		SPO^{DYS}	0.15	4.38
		SPO^{ILP}	0.15	23.53
		$SPO^{p=5\%}$	0.19	3.92
		SPO^{relax}	0.15	22.06
		$SqDE^{DYS}$	0.16	4.52
		MSE	0.17	0.24
		PFY	0.13	23.77
250	10	$Regret^{DYS}$	0.25	4.35
		SCE^{DYS}	0.10	4.25
		SPO^{DYS}	0.15	4.08
		SPO^{ILP}	0.15	28.85
		$SPO^{p=5\%}$	0.19	4.36
		SPO^{relax}	0.15	27.70
		$SqDE^{DYS}$	0.16	4.24
		MSE	0.17	0.27
		PFY	0.13	29.24

Table 7: Result on Capacitated Facility Location Problem Instances